UNIVERSITY OF OKLAHOMA

GRADUATE COLLEGE

ISOPERIMETRIC INEQUALITIES USING VAROPOULOS TRANSPORT

A DISSERTATION

SUBMITTED TO THE GRADUATE FACULTY

in partial fulfillment of the requirements for the

Degree of

DOCTOR OF PHILOSOPHY

By

ANTARA MUKHERJEE
Norman, Oklahoma
2008

Downloaded from SHAREOK. Persistent Handle URL: https://hdl.handle.net/11244/318815

ISOPERIMETRIC INEQUALITIES
USING VAROPOULOS TRANSPORT

A DISSERTATION APPROVED FOR THE
DEPARTMENT OF MATHEMATICS

BY

Dr. Noel Brady, Chair

Dr. Max Forester

Dr. Lucy Lifschitz

Dr. Krishnan Shankar

Dr. Sridhar Radhakrishnan

© Copyright by ANTARA MUKHERJEE 2008
All rights reserved.

THIS DISSERTATION IS DEDICATED

TO

My parents

Gautom Mukherjee, and

Tapasi Mukherjee

For always believing in me.

Acknowledgements

First, I wish to express my gratitude to my advisor, Dr Noel Brady, for introducing me to topology when I started graduate school, for his guidance and unconditional support during all these years, and for being an excellent mentor. I am grateful for having had the opportunity to work with him.

I also wish to thank all my committee members for supporting and me throughout my years as a graduate student, I have gained immensely from the classes I had with them.

I wish to extend my heart felt gratitude to my friend Taralee Mecham for the numerous hours she spent with me talking about math and life in general. I am especially indebted to her for letting me stay with her these last few months. My thanks to my friends Eduardo Martinez for enlightening me on various aspects of Math, Vera Tonić for being a great friend and Urmila Pal Chaudhuri for providing moral support.

Finally I would like to thank my family, my parents and aunt Mrs Ratna Chatterjee for always encouraging me and my husband Shankar Madhab Banik for always being understanding and supporting me no matter what.

Contents

1 Introduction **1**
- 1.1 History of Filling Functions 1
- 1.2 Goal of this thesis 3
- 1.3 Overview of proof of the main theorems 3
- 1.4 Organization of the Thesis 4

2 Basic Notions on Dehn Functions **6**
- 2.1 Dehn Functions 6
  - 2.1.1 **Geometric Interpretation of the Dehn function**. . . 9
- 2.2 Higher dimensional Dehn functions 14
  - 2.2.1 **Definitions and notations** 14
  - 2.2.2 **Results involving higher dimensional Dehn functions** 17

3 Transverse Maps, Handle Decompositions and Reduced Diagrams **21**
- 3.1 Background on Handle Decompositions 21
- 3.2 Handlebody Diagrams 23

4 Lower Bounds for Nil and Sol **32**
- 4.1 The connection between Linear Algebra and Cell Decomposition of Mapping Tori 32
  - 4.1.1 Cell Decomposition of the Mapping Torus A_T 33
- 4.2 The Lower Bounds 36

5 Upper Bounds- Reduction to Varopoulos Isoperimetric Inequality **47**
- 5.1 Definitions 47
- 5.2 Dual Graphs 48
  - 5.2.1 Definitions and Notations 52
  - 5.2.2 Reducing to Varopoulos Isoperimetric Inequality 54

6 Upper Bounds- Varopoulos Transport Argument **57**
6.1 The connection between Dehn functions and Varopoulos Isoperimetric Inequalities 58
6.2 Intuition behind the Varopoulos argument 61
6.3 The Transport Computation 63
6.4 Isoperimetric Inequalities for groups of Polynomial growth 69
6.4.1 **A 2-dimensional Example** 69
6.4.2 **A 3-dimensional Example** 70
6.5 Isoperimetric Inequalities for groups of Exponential growth 71

Chapter 1

Introduction

1.1 History of Filling Functions

This thesis contains results concerning Isoperimetric Inequalities of finitely presented groups. The complexity of the word problem has been the core of research for several Geometric Group Theorists for more than a hundred years now. In the 1910's Dehn realized that the problems with which he was trying to understand low-dimensional manifolds were examples of more general group-theoretic problems. In 1912 he proposed the three decision problems namely, the Word Problem, the Conjugacy Problem and the Isomorphism Problem in his famous paper [16]. In spite of his findings about the link between geometry and group theory, the connection between these two fields did not appear in the research of topologists until the 1960's when Roger Lyndon rediscovered the paper's main idea, where Dehn had used planar diagrams to study word problems. At the same time Weinbaum found E. van Kampen's work where the latter used planar 2-complexes or diagrams (now known as *van Kampen diagrams*) to study finitely presented groups. Later on in the 1980's and 1990's it was due to Gromov ([22]

and [23]) that the precise equivalence between filling functions of manifolds and complexity functions for word problems came to light.

The origin of the quest to find a link between topology and combinatorial group theory can be traced back to Belgian physicist Plateau's (1873, [32]) classical question whether every rectifiable Jordan loop in every 3-dimensional Euclidean space bounds a disc of minimal area. Since then geometers and topologists have been investigating various ways to obtain efficient fillings of spheres by minimal volume balls. Thanks to the efforts of Dehn [16] and Gromov [21] we now know that there is an intimate connection between this classical geometric problem and group theory. Various other results on Dehn functions can be found in papers by McCammond [27], Ol'shanskiĭ [30] and Rips [33]. The most significant development in this area has been Gromov's introduction of word hyperbolic groups.

Important results in the area of Dehn functions using different techniques also appear in the pair of following papers, the first in 1997 (published in 2002) by Sapir, Birget and Rips ([35]) and the second in 2002 by Birget, Ol'shanskiĭ, Yu, Rips and Sapir, ([5]). They showed that there exists a close connection between Dehn functions and complexity functions of Turing machines. One of their main results said that the Dehn function of a finitely presented group is equivalent to the time function of a two-tape Turing machine. More of this history and background on isoperimetric inequalities can be found in the paper by Bridson in [13].

Since the 1990's topologists have been interested in Dehn functions in higher dimensions. Gromov [23], Epstein et al.[17], first introduced the higher order Dehn functions and Alonso et al. [3] and Bridson [11] produced the first few results in the context of these functions. In this thesis we have results on second

order Dehn functions for lattices of the 3-dimensional Nil and Sol geometries.

1.2 Goal of this thesis

In the main theorems of this thesis we provide upper and lower bounds of the second order Dehn functions for 3-dimensional groups Nil and Sol.

Theorem 1.1 (A. Mukherjee)**.** *The second order Dehn function (denoted by $\delta^{(2)}$) of the lattices in the Nil geometry is given by $\delta^{(2)}(n) \sim n^{\frac{4}{3}}$.*
In other words, second order Dehn function of the groups $\mathbb{Z}^2 \rtimes_\phi \mathbb{Z}$, where ϕ has eigenvalues ± 1 and has infinite order, is given by, $\delta^{(2)}(n) \sim n^{\frac{4}{3}}$.

Theorem 1.2 (A. Mukherjee)**.** *The second order Dehn function (denoted by $\delta^{(2)}$) of the lattices of the 3-dimensional geometry Sol is given by $\delta^{(2)}(n) \sim n\ln(n)$.*
In other words, that the second order Dehn functions for the groups $\mathbb{Z}^2 \rtimes_\phi \mathbb{Z}$, where the eigenvalues of ϕ are not ± 1, $\delta^{(2)}(n) \sim n\ln(n)$.

1.3 Overview of proof of the main theorems

The main goal of this thesis is to obtain upper and lower bounds of second order Dehn function in case of groups mentioned in the theorems above.

We will show that $\delta^{(2)}(n) \succeq n^{\frac{4}{3}}$ for the lattices in the Nil geometry and $\delta^{(2)}(n) \succeq n\ln(n)$ in case of lattices in the Sol geometry. To establish a lower bound in each of these cases, we will exhibit a sequence of embedded 3-balls and their boundary 2-spheres such that the volume growth of the 3-balls is as large as possible relative to the growth of boundary area.

Next, in order to obtain upper bounds, we start with a reduced, transverse diagram $f : (D^3, S^2) \to K$, where D^3 is a 3-ball, S^2 is its boundary sphere and K

is the 3-dimensional ambient space. We then define a dual Cayley graph Γ in the ambient space K where each vertex of Γ is a 3-cell in K and each edge is a 2-cell common to two adjacent 3-cells. Now, we consider a finite subset of vertices D of Γ corresponding to the 0-handles of the diagram mapped into K and we define an integer-valued function $\phi_D : \Gamma^{(0)} \to \mathbb{Z}^+$ with finite support i.e, $\phi_D(\alpha) =$ number of pre-images of α in (D^3, S^2) for all $\alpha \in D$, otherwise $\phi_D(\alpha) = 0$. This leads us to the fact that the volume of the 3-ball D^3 and $||\phi_D|| = \sum_{\sigma \in D} \phi_D(\sigma)$ are equal. The boundary of D according to Varopoulos is $\partial_V D = \{\tau : \tau$ is a face of two 3-cells, $\sigma_i, \sigma_j; \phi_D(\sigma_i) \neq \phi_D(\sigma_j)\}$, next we define $\| \nabla\phi_D \| = \sum_{\tau \in \partial_V D} |\phi_D(t(\tau)) - \phi_D(i(\tau))|$, where i, t are functions which determine the initial and terminal vertices of an edge in Γ. This function gives the number of edges in the boundary $\partial_V D$. In fact, we can show that $\| \nabla\phi_D \| \leq Vol^2(S^2)$. Therefore the problem of upper bound reduces to an inequality involving $||\phi_D||$ and $\| \nabla\phi_D \|$ provided $Vol^3(D^3) = ||\phi_D||$ and $Vol^2(S^2) \geq ||\nabla\phi_D||$.

Finally, we show that $||\phi_D|| \leq ||\nabla\phi_D||^{\frac{4}{3}}$ for the lattices in the 3-dimensional geometry Nil and $||\phi_D|| \leq ||\nabla\phi_D|| \ln(||\nabla\phi_D||)$ for the lattices in the 3-dimensional geometry Sol using a variation the Varopoulos transport argument.

1.4 Organization of the Thesis

This thesis is organized as follows, in the second chapter we introduce ordinary Dehn functions as well as higher order Dehn functions and discuss results involving higher order Dehn functions.

In the third chapter we give a survey of generalized handle body diagrams in 2 and 3-dimensions which can be thought of as higher dimensional analogs of van Kampen diagrams. We use transverse maps for this and the main result here

is to show that a reduced diagram can be obtained from an unreduced diagram without changing the map on the boundary. Reduced diagrams are a key to obtaining upper bounds for second order Dehn function.

The fourth chapter introduces the structure of the 3-manifolds which are torus bundles over the circle. We then describe the cell decomposition of the torus bundles and introduce the notion of dual graphs in the cell decomposition. Finally we focus on the main examples of this thesis which are lattices in the 3-dimensional geometries Nil and Sol and obtain the lower bounds of the second order Dehn function in both these cases.

The main result in the fifth chapter is that the isoperimetric inequality involving $Vol^3(D^3)$ and $Vol^2(S^2)$ reduces to an inequality between $||\phi_D||$ and $||\nabla\phi_D||$. We do this by defining a dual graph in the ambient space.

In the sixth chapter we use the Varopoulos transport argument to obtain the upper bounds of second order Dehn functions in case of both Nil and Sol.

Chapter 2

Basic Notions on Dehn Functions

In this section we introduce some basic definitions on ordinary and higher dimensional Dehn functions. We also present a short survey of results involving higher dimensional later in the chapter. The definitions were primarily taken from [13] and [6].

2.1 Dehn Functions

Definition 2.1. (*Dehn function*). Let $\mathcal{P} = \langle \mathcal{A} \mid \mathcal{R} \rangle$ be the finite presentation of a group G, where $\mathcal{A}$ denotes the set of generators and $\mathcal{R}$ denotes the set of all relators.

We can define the *Dehn function* of $\mathcal{P}$ in the following way: ([13])

Given a word $w = 1$ in generators $\mathcal{A}^{\pm 1}$,

$Area(w) = \min\{N_w \in \mathbb{N} : \exists \text{ an equality } w = \prod_{i=1}^{N_w} x_i r_i x_i^{-1}; x_i \in F(\mathcal{A}) \text{ and } r_i \in \mathcal{R}\}$,

here $F(\mathcal{A})$ denotes the free group on the generating set $\mathcal{A}$.

The *Dehn function* of $\mathcal{P}$ is $\delta_{\mathcal{P}}(n) = \max\{Area(w) : |w| \leq n\}$.

Example 2.2. The group of integers $\mathbb{Z}$ can be expressed as the finite presentation

$\langle a \mid \rangle$, so the Dehn function for this presentation is $\delta(n) \equiv 0$. If we use the finite presentation $\langle a, b \mid b \ \rangle$ for $\mathbb{Z}$, $\delta(n) = n$. In fact, for any positive integer k, there is a presentation of $\mathbb{Z}$ which has a Dehn function kn. For example, given the presentation $\langle a, b, c \mid a, ab^{-1} \rangle$, the Dehn function is $\delta(n) = 2n$, next, given a positive integer k, the Dehn function for $\langle a_1, a_2, ..., a_k, t \mid a_1, a_i a_{i+1}^{-1}; i = 1, 2, .., k-1 \rangle$ is given by, $\delta(n) = kn$.

Thus this example where different presentations of the same group gives rise to different Dehn functions, raises the question of equivalence in Dehn functions.

Definition 2.3. (*Equivalent Functions*). Two functions $f, g : [0, \infty) \to [0, \infty)$ are said to be $\sim$ equivalent if $f \preceq g$ and $g \preceq f$, where $f \preceq g$ means that there exists a constant $C > 0$ such that $f(x) \leq Cg(Cx) + Cx$, for all $x \geq 0$, (and modulo this equivalence relation it therefore makes sense to talk of "the" Dehn function of a finitely presented group). This equivalence is called *coarse Lipschitz equivalence.*

Proposition 2.4 (Gersten, [19])**.** *If the groups defined by two finite presentations are isomorphic, the Dehn functions of those presentations are $\sim$ equivalent.*

More generally, Alonso ([4]) showed that the Dehn functions of two quasi isometric groups are equivalent.

Dehn Function vs Isoperimetric Function

Definition 2.5. (*Isoperimetric Function of a Group*). A function $f : \mathbb{N} \to \mathbb{N}$ is an *isoperimetric function* for a group G if the Dehn function $\delta_{\mathcal{P}} \preceq f$ for some (and hence any) finite presentation $\mathcal{P}$ of G.

Given a smooth, closed, Riemannian manifold M, in the rest of this section we shall describe the isoperimetric function of M and discuss its relationship with the Dehn function of the fundamental group $\pi_1(M)$ of M.

Let $c : S^1 \to M$ be a null-homotopic, rectifiable loop and define $FArea(c)$ to be the infimum of the areas of all Lipschitz maps $g : D^2 \to X$ such that $g|_{\partial D^2}$ is a reparametrization of c.

Note that the notion of area used here is the same as that of area in spaces introduced by Alexandrov [1]. The basic idea is to define the area of a surface (or area of a map $g : D^2 \to X$) to be the limiting area of approximating polyhedral surfaces built out of Euclidean triangles.

Note 2.6. Given two metric spaces (X, d_X) and (Y, d_Y), where d_X denotes the metric on the set X and d_Y is the metric on set Y (for example, Y might be the set of real numbers $\mathbb{R}$ with the metric $d_Y(x, y) = |x-y|$, and X might be a subset of $\mathbb{R}$), a function $f : X \to Y$ is called *Lipschitz continuous* if there exists a real constant $K \geq 0$ such that, for all x_1 and x_2 in X, if $d_Y(f(x_1, x_2)) \leq K d_X(x_1, x_2)$. The smallest such K is called the Lipschitz constant of the function.

Definition 2.7. (*Isoperimetric or Filling function*) Let M be a smooth, complete, Riemannian manifold. The genus zero, 2-dimensional, isoperimetric function of M is the function $[0, \infty) \to [0, \infty)$ defined by,
$Fill_0^M(l) := sup\{FArea(c) \mid c : S^1 \to M$ null-homotopic, $length(c) \leq l\}$.

The Filling Theorem provides an equivalence between Dehn function and the Filling function defined above.

Theorem 2.8 (Filling Theorem, Gromov [21], Bridson, [13])**.** *The genus zero, 2-dimensional isoperimetric function $Fill_0^M$ of any smooth, closed, Riemannian*

manifold M is $\sim$ equivalent to the Dehn function $\delta_{\pi_1 M}$ of the fundamental group of M.

Example 2.9. Here are a few examples of manifolds and their Dehn functions.

1. The Dehn function of the fundamental group of a compact 2-manifold is linear except for the torus and the Klein bottle when it is quadratic.

2. The groups that interest us are fundamental groups of 3-manifolds and the Dehn functions of these groups can be characterized using the following theorem by Epstein and Thurston.

   Let M be a compact 3-manifold such that it satisfies Thurston's geometrisation conjecture ([38]).

   The Dehn function of $\pi_1(M)$ is linear, quadratic, cubic or exponential. It is linear if and only if $\pi_1(M)$ does not contain $\mathbb{Z}^2$. It is quadratic if and only if $\pi_1(M)$ contains $\mathbb{Z}^2$ but does not contain a subgroup $\mathbb{Z}^2 \rtimes_\phi \mathbb{Z}$ with $\phi \in GL(2,\mathbb{Z})$ of infinite order. Subgroups $\mathbb{Z}^2 \rtimes_\phi \mathbb{Z}$ arise only if a finite-sheeted covering of M has a connected summand that is a torus bundle over the circle, and the Dehn function of $\pi_1(M)$ is cubic only if each such summand is a quotient of the Heisenberg group.

2.1.1 Geometric Interpretation of the Dehn function.

The connection between maps of discs filling loops in CW complexes (or in other words a geometric interpretation of the Dehn function defined above) and the algebraic method of reducing words can be explained by any one of the following,

- van Kampen diagrams,
- pictures and,

- Handle body diagrams.

1. *van Kampen diagram.*

   Definition 2.10. (*van Kampen diagram*, [9]). Given a finite presentation $\mathcal{P} = \langle \mathcal{A} \mid \mathcal{R} \rangle$ of a group, let $Cay^2(\mathcal{P})$ denote the Cayley 2-complex corresponding to $\mathcal{P}$ (the Cayley 2-complex is the universal cover of the presentation 2-complex of $\mathcal{P}$ which has the Cayley graph as its 1-skeleton). A *van Kampen diagram* for a word $w \in \mathcal{F}(\mathcal{A})$ such that $w = 1$, is a combinatorial map $\pi : \triangle \to Cay^2(\mathcal{P})$, where $\triangle$ is a connected, simply connected, planar 2-complex and the word around the boundary of $\triangle$, (starting from a base vertex), reads w.

   The planar 2-complex $\triangle$ in the definition above is referred to as the van Kampen diagram for w over the presentation $\mathcal{P}$.
   van Kampen's lemma provides a necessary and sufficient condition for the existence of a van Kampen diagram.

   Lemma 2.11 (van Kampen's Lemma, [26])**.** *Given a finite presentation $\mathcal{P} = \langle \mathcal{A} \mid \mathcal{R} \rangle$ of a group Γ, let w be a word in $\mathcal{F}(\mathcal{A})$.*

   - *$w = 1$ in $\mathcal{P}$ if and only if there exists a van Kampen diagram for w over $\mathcal{P}$.*
   - *Moreover, if $w = 1$ in Γ then, $Area(w) = min \{ Area (\triangle) \mid \triangle$ is a van Kampen diagram for w over $\mathcal{P}\}$, where $Area(\triangle)$ is the number of 2-cells in $\triangle$.*

2. *Pictures.*

Definition 2.12. (*Pictures*, [9]) Consider the presentation $\mathcal{P} = \langle \mathcal{A} \mid \mathcal{R} \rangle$, the standard complex $\mathcal{K}^2(\mathcal{P})$ and $w \in \langle\langle \mathcal{P} \rangle\rangle$ (the normal closure of $\mathcal{R}$). Then w defines a path γ_w in the 1-skeleton $\mathcal{K}^2(\mathcal{P})^{(1)}$ which is null-homotopic in $\mathcal{K}^2(\mathcal{P})$. This means that there is a map $f : (D, \partial D) \to (\mathcal{K}^2(\mathcal{P}), \mathcal{K}^2(\mathcal{P})^{(1)})$ such that $f|_\partial D = \gamma_w$. The *picture* corresponding to f is the disc D together with the collection of subdisks (or "fat vertices") V_i and the embedded loops and arcs. Each arc and loop is transversely oriented and labeled by some $a \in \mathcal{A}$, inducing labels r_i on the boundary of each V_i, and a label w on ∂D, when read from appropriate points, and in an appropriate direction.

The pictures are dual to the van Kampen diagrams in the sense that each compact region (interior of a 2-cell) in the diagram is a subdisk, dual to each edge separating any two faces in the diagram we insert an arc joining the two adjacent subdisks. Finally we label and transversely orient these arcs according to the orientations of the original edges in the diagram.

3. *Handle body diagrams.*

Definition 2.13. (*i-Handle, [14]*) An index i-handle is written as $H^i = \Sigma^i \times D^{n-i}$, where Σ^i is a connected i-manifold (we will consider $\Sigma^i = D^i$ in all our examples) and D^{n-i} is a $(n-i)$ closed disk.

Definition 2.14. (*Generalized handle decomposition or Handlebody diagrams, [14]*) A handle decomposition of an n-manifold M is a representation of the manifold as a filtration $M_0 \subset M_1 \subset ..... \subset M$ where each M_i is obtained from M_{i-1} by attaching finitely many i-handles.

Note that handle decompositions are never unique. A detailed discussion on handle body diagrams is provided in Section 3. This technique proves to

be most efficient when used to geometrically interpret higher dimensional Dehn functions discussed below.

The following example provides an illustration of the diagrams and pictures mentioned above and helps bring out the relation between the three.

Example 2.15. The following Figure (2.1) is an illustration of all the three diagrams and pictures mentioned above.

Part (i) is the handle body diagram, the numbers in the figure are labels of 0, 1 or 2-handles. The 0-handles are $2n$-sided polyhedral 2-discs where n denotes the number of sides of 2-cells in the van Kampen diagram, (ii), in this example the 2-cells are either triangular or quadrilateral, so this means the 0-handles are hexagonal or octagonal discs and each 0-handle corresponds to each 2-cell in the diagram. A 1-handle is homeomorphic to a rectangle $(= I \times I)$ which has two 0-handles glued to $\{0\} \times I$ and $\{1\} \times I$ or in some cases one 0-handle glued to one side while the other side goes to the boundary.

Part (ii) in the figure is the van Kampen diagram with boundary word reading $abcdefgh$, part (iii) is the picture obtained in the following way from the van Kampen diagram. The subdisks in the picture (iii) are dual to the faces in (ii), the arcs joining the subdisks are transverse to the edges in the van Kampen diagram and the labels and orientations transverse to the arcs correspond to the labels in (ii) .

The map ϕ from the handle-body diagram to the van Kampen diagram is the 2-handle collapse to vertices together with the (horizontal) 1-handle collapse to edges.

The other map φ on the other hand goes from the handle-body diagram to the picture which is a (vertical) 1-handle collapse to the arcs. Hence the labels

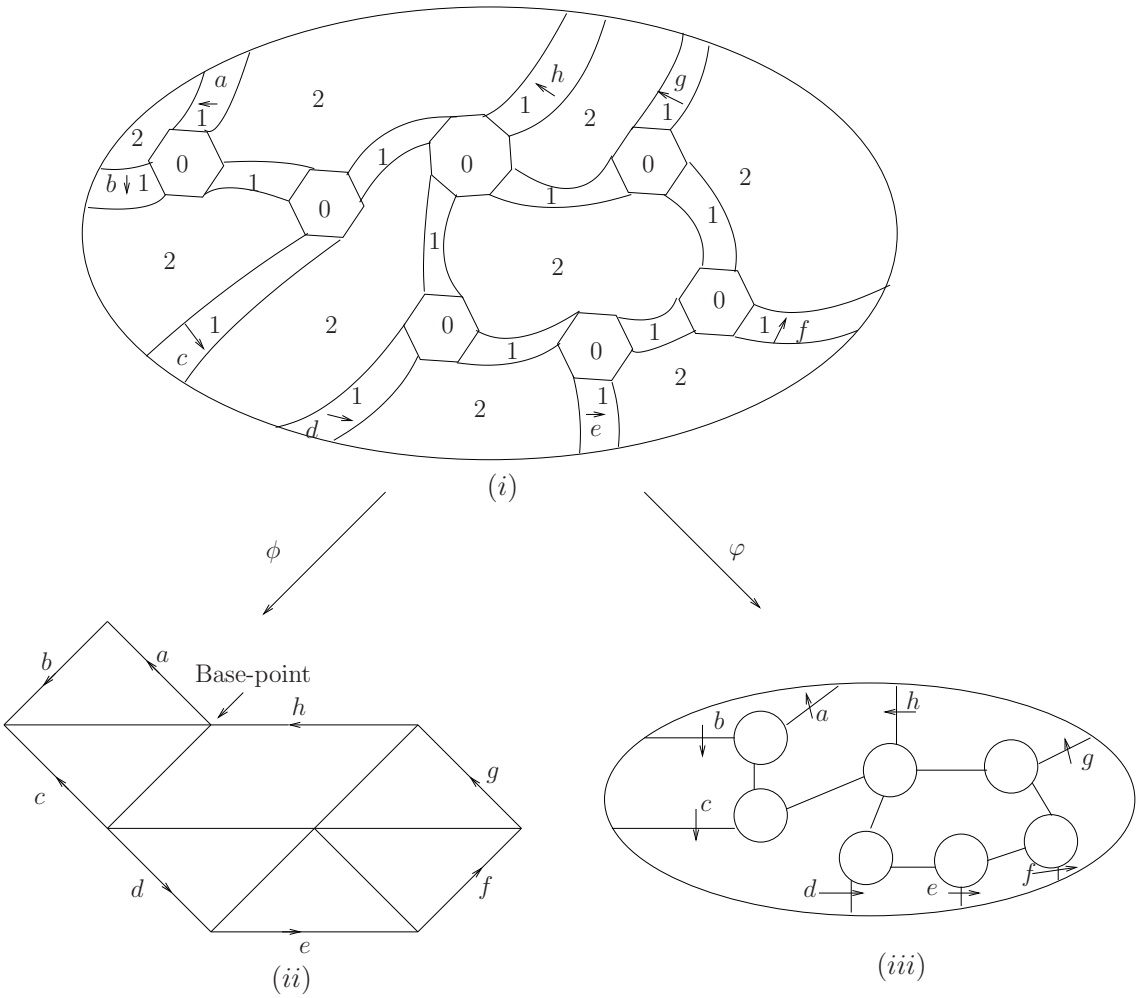

Figure 2.1: (i) Handle body diagram, (ii) van Kampen diagram, and (iii) corresponding Picture

a, b, c etc. in the 1-handles of (iii), become transverse orientations on the arcs of the picture (ii).

2.2 Higher dimensional Dehn functions

2.2.1 Definitions and notations

Epstein et al. [17] and Gromov [23] first introduced higher dimensional Dehn functions at about the same time. However later, Alonso *et al.* [3] and Bridson [11] provided equivalent definitions which were different from the two mentioned above. In the discussion on higher dimensional Dehn functions presented here we will be using Brady *et al*'s ([6]) definition which is based on the prior definitions given by Bridson and Alonso *et al.* Before we introduce higher dimensional Dehn functions we note the definition of groups of type $\mathcal{F}_n$. We also explain below the reason groups of this type are important in the discussion of higher dimensional Dehn functions.

Definition 2.16. (*Eilenberg-Maclane complex*, [12]) The Eilenberg-Maclane complex (or classifying space) $K(\Gamma, 1)$ for a group Γ is a CW complex with fundamental group Γ and contractible universal cover. Such a complex always exists and its homotopy type depends only on Γ.

Definition 2.17. (*Finiteness property* $\mathcal{F}_n$, [40]) A group Γ is said to be of type $\mathcal{F}_n$ if it has an Eilenberg-Maclane complex $K(\Gamma, 1)$ with finite n-skeleton. Clearly a group is of type $\mathcal{F}_1$ if and only if it is finitely generated and of type $\mathcal{F}_2$ if and only if it is finitely presented.

Note 2.18. It is necessary to consider finite presentation of the groups in the context of Dehn functions since, if we have an infinite presentation the Dehn

function turns out to be rather uninteresting and in some extreme cases even a constant.

For example, let $1 \to N(G) \to F_A \to G \to 1$ be a short exact sequence for a group G, where F_A is a free group on a generating set A for G and $N(G)$ the normal closure of G. Now if we consider the infinite presentation $\langle A \mid N(G)\rangle$, then the Dehn function $\delta(x) = \max\{Area(w) \mid w \text{ is a word in } G, |w| \leq x\} = 1$, a constant function, for all x.

Intuitively, the *k-dimensional Dehn function*, $k \geq 1$, is the function $\delta^{(k)} : \mathbb{N} \to \mathbb{N}$ defined for any group G which is of type $\mathcal{F}_{k+1}$ and $\delta^{(k)}(n)$ measures the number of $(k+1)$-cells that is needed to fill any singular k-sphere in the classifying space $K(G,1)$, comprised of at most n k-cells. Up to equivalence the higher dimensional Dehn functions of groups are quasi-isometry invariants.

The following part of this section is devoted to the technical definition of higher dimensional Dehn function given by Brady *et al.*, ([6]).

Notation 2.19. Henceforth we will denote an n-dimensional disc (or ball) by D^n and an n-dimensional sphere by S^n.

Definition 2.20. (*Admissible maps*) Let W be a compact k-dimensional manifold and X a CW complex, an admissible map is a continuous map $f : W \to X^{(k)} \subset X$ such that $f^{-1}(X^{(k)} - X^{(k-1)})$ is a disjoint union of open k-dimensional balls, each mapped by f homeomorphically onto a k-cell of X.

Definition 2.21. (*Volume of f*) If $f : W \to X$ is admissible we define the volume of f, denoted by $Vol^k(f)$, to be the number of open k-balls in W mapping to k-cells of X.

Given a group G of type $\mathcal{F}_{k+1}$, fix an aspherical CW complex X with fundamental group G and finite $(k+1)$-skeleton. Let $\widetilde{X}$ be the universal cover of

X. If $f : S^k \to \widetilde{X}$ is an *admissible* map, define the *filling volume* of f to be the minimal volume of an extension of f to D^{k+1} in the following way,

$\text{FVol}(f) \ = \ \min\{Vol^{k+1}(g) \mid g : D^{k+1} \to \widetilde{X}, g|_{\partial D^{k+1}} = f\}$,

then, $k-$dimensional Dehn function of X is

$\delta^{(k)}(n) \ = \ \sup\{ \text{FVol}(f) \mid f : S^k \to \widetilde{X}, Vol^k(f) \leq n\}$.

Remark 2.22. Here are a few observations regarding higher dimensional Dehn functions,

1. Up to equivalence, $\delta^{(k)}(n)$ is a quasi-isometry invariant.

2. In the above definitions it is possible to use X in place of $\widetilde{X}$ since $f : S^k \to X$ (or $f : D^{k+1} \to X$) and their lifts to $\widetilde{X}$ have the same volume.

All the groups discussed in this thesis is at most 3-dimensional so we will restrict k in the above definitions such that $k \leq 2$.

The following are examples of second order Dehn functions.

Example 2.23. (*Examples of groups and their second-order Dehn functions*):

1. By definition,the second order Dehn function of a 2-complex with contractible universal cover is linear.

2. The second order Dehn function of any group of every (word) hyperbolic group H is linear and so is the direct product of H with any finitely generated free group, both these results were established by Alonso *et al.* in [2].

3. The following is a result by Bridson on the second order Dehn function of HNN extensions.

Theorem 2.24 (M. Bridson, [11]). *(a) The second order Dehn function of any HNN extension of $\mathbb{Z}^2$ with finitely many stable letters is $\preceq n^2$.*

(b) The second order Dehn function of any HNN extension of $\mathbb{Z}^3$ with finitely many stable letters is $\preceq n^3$, provided that the amalgamated subgroups are all of infinite index in $\mathbb{Z}^3$.(Note that here $\preceq$ means up to a coarse Lipschitz equivalence.)

4. The second order Dehn function of any finitely generated abelian group with torsion-free rank greater that two is $\sim n^{3/2}$, e.g, $\mathbb{Z}^3$ ([41]).

2.2.2 Results involving higher dimensional Dehn functions

Over the last decade there has been a considerable research that has led to a better understanding of higher dimensional Dehn functions. We start with the paper by Alonso *et al.* ([3]) where they talk about higher dimensional volume and filling volume of CW complexes and also discuss the link between Dehn functions of complexes and Dehn functions of groups. One of the important results proved by them is that if two k-connected combinatorial complexes admit discrete cocompact group actions and are quasi-isometric then their higher dimensional Dehn functions are equivalent. They use pictures which are dual to higher dimensional analogs to van Kampen diagrams in order to prove the results in this paper.

In another 1999 paper Wang and Pride ([42]) provided upper and lower bounds for second-order Dehn functions of HNN extensions, and then they use this to establish the existence of superquadratic second order Dehn functions. They show that for any positive integer r, there is a group G_r such that $\delta^{(2)}_{G_r}$ lies between $n^{\frac{r}{2}+1}$ and n^{r+1}.

In 2000, N. Brady and M. Bridson [7] had proved the following theorem on

the isoperimetric spectrum of second order Dehn functions. The k-dimensional isoperimetric spectrum ($k \geq 1$) is given by,

$IP^{(k)} = \{\alpha \in [1, \infty) \mid f(x) = x^{\alpha}$ is equivalent to a k-dimensional Dehn function$\}$.

Theorem 2.25 (N. Brady and M. Bridson, [7]). *For each pair of positive integers, $p \geq q$,there exists a finitely presented group whose second order Dehn function $\sim n^{2-\frac{1}{\alpha}}$, where $\alpha = 2\log_2(2p/q)$. In particular, the spectrum of exponents of second order Dehn functions is dense in $[3/2, 2]$.*

In 2002 Wang published the article ([41]) where he provided upper and lower bounds of second-order Dehn functions of some split extensions of the form $\mathbb{Z}^2 \rtimes_{\phi} \mathbb{Z}$. He used spherical pictures of second homotopy module of the group presentations in order to obtain the bounds. The main result of Wang's 2002 paper is given below:

Theorem 2.26 (X. Wang, [41]). *Denote the second order Dehn function of the split extensions $\mathbb{Z}^2 \rtimes_{\phi} \mathbb{Z}$ by $\delta^{(2)}_{\mathbb{Z}^2 \rtimes_{\phi} \mathbb{Z}}$.*

1. *If ϕ has finite order, then $\delta^{(2)}_{\mathbb{Z}^2 \rtimes_{\phi} \mathbb{Z}} \sim n^{\frac{3}{2}}$.*
2. *If ϕ has eigenvalues ± 1 and has infinite order, then $n^{\frac{4}{3}} \preceq \delta^{(2)}_{\mathbb{Z}^2 \rtimes_{\phi} \mathbb{Z}} \preceq n^{\frac{3}{2}}$.*
3. *If the eigenvalues of ϕ are not ± 1, then $\delta^{(2)}_{\mathbb{Z}^2 \rtimes_{\phi} \mathbb{Z}} \succeq n\,ln(n)$.*

Remark 2.27. In 1983 Pansu [31] provides a proof for isoperimetric inequalities for 3-dimensional Heisenberg group i.e, the group (ii) above, in the case where $\phi \in SL_2(\mathbb{Z})$ is represented by $\begin{pmatrix} 1 & 1 \\ 0 & 1 \end{pmatrix}$. Here is the main theorem of the paper.

Let G be the 3-dimensional Heisenberg group i.e, the group of upper triangular matrices $\begin{pmatrix} 1 & \alpha & \beta \\ 0 & 1 & \gamma \\ 0 & 0 & 1 \end{pmatrix}$*, where α, β, γ are real entries. Let g be a left invariant metric on G. Then, for any domain $D \subset G$, one has $vol(D) \leq const(g)\, vol(\partial D)^{4/3}$.*

But a geometric interpretation of Pansu's proof in the context of higher dimensional Dehn functions mentioned in the previous section implies that the isoperimetric inequality given in the theorem above holds only for *embedded* balls and spheres .

In [41], Wang refers to the Coulhon and Saloff-Coste paper [15] for the upper bound in part (iii), but again the results of [15] holds in the case of *embedded* balls and spheres.

So the following is a natural question and the main purpose of this research was to investigate it thoroughly.

Problem 2.28. *Show that the second-order Dehn functions for groups mentioned in Wang's result above are the following:*
For part (ii), $\delta^{(2)}_{\mathbb{Z}^2 \rtimes_\phi \mathbb{Z}} \sim n^{\frac{4}{3}}$
For part (iii), $\delta^{(2)}_{\mathbb{Z}^2 \rtimes_\phi \mathbb{Z}} \sim n\, ln(n)$.

More recently in 2005, Brady, Bridson, Forester and Shankar, ([6]), proved a number of results on k-dimensional isoperimetric spectrum. One of the main results of the paper is mentioned below. This result is obtained by investigating higher dimensional Dehn functions of products $G \times \mathbb{Z}$.

Theorem 2.29 (Brady, Bridson, Forester and Shankar, [6])**.** *Let $IP^{(k)}$ be the k-isoperimetric spectrum defined above, then $\mathbb{Q} \cap [(k+1)/k, \infty) \subset IP^{(k)}$.*

The paper by Brady and Forester, ([8]) on the density of isoperimetric spectra is the latest in the list of articles in this fast developing area of geometric group theory. The examples they discuss here are similar to one of the examples in this thesis, namely Sol but the matrices corresponding to the groups here have determinant > 1. The main result of this article is,

Theorem 2.30 (Brady and Forester, [8])**.** *$IP^{(k)}$ is dense in $[1, \infty)$ for $k \geq 2$.*

As seen in this chapter, there has been a lot of research where higher dimensional Dehn functions are concerned since the 1990's. Over the years geometric group theorists have provided answers to old questions using machinery that suitably fits the context of the problems. In this thesis we will provide solutions to two well known problems on second order Dehn functions using a version of Varopoulos transport argument and handle body diagrams by Buoncristiano, Rourke and Sanderson.

Chapter 3

Transverse Maps, Handle Decompositions and Reduced Diagrams

In this chapter we will discuss generalized handle decompositions which will help us compute upper bounds for higher dimensional Dehn functions in specific cases later in the thesis.

3.1 Background on Handle Decompositions

Any compact, smooth or piecewise linear manifold, admits a handle decomposition ([28], [34]), also each handle decomposition can be made proper (see details in [34]). In 1961 S. Smale [36], established the existence of exact handle decompositions of simply connected and cobordisms of dimensionality $n \geq 6$. In the former paper by Smale he defines the handlebodies, the elements of $\mathfrak{H}(n, k, s)$ in the following way, if $H \in \mathfrak{H}(n, k, s)$, then H is defined by attaching k number of

s-discs, to an n-disc and thickening them. Then, he proved a number of results on handle decompositions like the theorem given below, which gives the Heegaard decomposition in case of 3-manifolds.

Theorem 3.1. *Let M be a closed $C^\infty(2m+1)$-manifold which is $(m-1)$-connected. Then $M = H \cup H'$, $H \cap H' = \partial H = \partial H'$ where $H, H' \in H \in \mathfrak{H}(2m+1, k, m)$ are handlebodies (∂V means boundary of manifold V).*

The handlebody theorem is one of the important results of this paper which states that:

Theorem 3.2. *Let $n \geq 2s+2$ and if $s = 1, n \geq 5$; let $H \in \mathfrak{H}(n, k, s)$, and let $V = \chi(H; f_1, ..., f_r; s+1)$ be another smooth manifold obtained by attaching to H copies of $D_i^s \times D_i^{r-s}$ using the attaching maps f_i, also note that $\pi_s(V) = 0$. In addition, if $s = 1$, assume $\pi_1(\chi(H; f_1, ..., f_{r-k}; 2)) = 1$. Then $V \in \mathfrak{H}(n, r-k, s+1)$.*

Note that the attaching maps mentioned above $f_i : \partial D_i^s \times D_i^{r-s} \to \partial H$ for $i = 1, 2, .., k$ are imbeddings with disjoint images for $s \geq 0$ and $n \geq s$.

At about the same time in his article ([37]), Stallings pointed out a gap in the handlebody theorem for the case $s = 1$.

In this thesis we will be using the generalized handle decomposition of manifolds, mainly due to Buoncristiano, Rourke, Sanderson, [14]. This reference by Buoncristiano, Rourke, Sanderson ([14]) is a lecture series on a geometric approach to homology theory.

Here they introduce the concept of transverse CW complexes. These complexes have all the same properties of ordinary cell complexes. The result from this article which we will be using in this thesis is known as the Transversality Theorem, and using this theorem any continuous map may be homotoped to a

transverse map (Definition 3.8). Here is the statement of the Transversality theorem and is used to show the maps from the handle decompositions we construct to the ambient space are transverse.

Theorem 3.3 (Buoncristiano, Rourke and Sanderson, [14])**.** *Suppose X is a transverse CW complex (a CW complex is transverse if each attaching map is transverse to the skeleton to which it is mapped), and $f : M \to X$ is a map where M is a compact piecewise linear manifold. Suppose $f\ |_{\partial M}$ is transverse, then there is a homotopy of f rel ∂M to a transverse map.*

In fact, if M is a generalized handle decomposition i.e, it is constructed from another manifold with boundary M_0, by attaching finite number of generalized handles, then the map f itself is homotopic to a transverse map. Handles are still the same as handlebodies, defined above in the Smale case and they are attached to M_0 via the boundaries of the handles.

3.2 Handlebody Diagrams

The following definitions and statement of Transversality theorem were taken from the lecture notes for a course [18] taught by Max Forester.

Definition 3.4. (*Index i-Handle*) An index i-handle is written as $H^i = \Sigma^i \times D^{n-i}$, where Σ^i is a connected i-manifold (we will consider $\Sigma^i = D^i$ in all our examples) and D^{n-i} is a $(n-i)$ closed disk.

Note 3.5. The boundary of a i-handle is $\partial H^i = \partial\Sigma^i \times D^{n-i} \cup \Sigma^i \times \partial D^{n-i}$.

Given an n-manifold M_0 with boundary and an i-handle H^i, let $\phi : \partial\Sigma^i \times D^{n-i} \to \partial M_0$ be an embedding. Form $M_0 \cup_\phi H^i$ a new manifold with boundary

obtained from M_0 by attaching an i-handle in the following way, $(M_0 \amalg H^i)/(x \sim \phi(x), \forall x \in \partial\Sigma^i \times D^{n-i})$.

Definition 3.6. (*Generalized Handle Decomposition*) A generalized handle decomposition of M is a filtration: $\emptyset = M^{(-1)} \subset M^{(0)} \subset M^{(1)} \subset ..... \subset M^{(n)} = M$ such that:

- Each $M^{(i)}$ is a codimension-zero submanifold of M. ($L \subset M$ is a codimension-zero submanifold if L is an n-manifold with boundary and ∂L is a submanifold of M.)
- $M^{(i)}$ is obtained from $M^{(i-1)}$ by attaching finitely many i-handles.

Remark 3.7. In case M is a compact n-manifold with boundary denoted by, ∂M, then the generalized handle decomposition of M is:

- A generalized handle decomposition of ∂M, namely: $\emptyset = N^{(-1)} \subset N^{(0)} \subset N^{(1)} \subset ..... \subset N^{(n-1)} = \partial M$, where each $M^{(i)}$ is a codimension-zero submanifold of ∂M
- A filtration of M, $\emptyset = M^{(-1)} \subset M^{(0)} \subset M^{(1)} \subset ..... \subset M^{(n)} = M$ where each $M^{(i)}$ is a codimension-zero submanifold of M and $M^{(i)}$ is obtained from $M^{(i-1)} \cup N^{(i-1)}$ by attaching i-handles.
- Each $(i-1)$-handle of N is a connected component of the intersection of N with an i-handle of M (this means that $N^{(i-1)} = \partial M \cap M^{(i)}$).

Definition 3.8. (*Transverse Maps*) Let M be a compact n-manifold and X a cell-complex. A continuous map $f : M \to X$ is *transverse* if M has a generalized handle decomposition such that for every handle $H^i = \Sigma^i \times D^{n-i}$ in M, the restriction $f\mid_{H^i}: \Sigma^i \times D^{n-i} \to X$ is given by $\phi \circ pr_2$ where $pr_2 : \Sigma^i \times D^{n-i} \to D^{n-i}$

is a projection map to the second coordinate and ϕ is the characteristic map of an $(n-i)$-cell of X. We will refer to the generalized handle decomposition of M as a *handle body diagram* or just a *diagram.*

Note 3.9. An i-handle maps to a $(n-i)$-cell this implies, $f(M) \subset X^{(n)} = X$.

Definition 3.10. (*"good" CW complex*) A CW complex is "good" if and only if, each attaching map is transverse to the skeleton to which it is mapped.

Next we have a version of the Transversality theorem which we will refer to later in this thesis.

Theorem 3.11 (Transversality Theorem [14])**.** *If X is an n-dimensional, "good" CW complex and M is a genaralized handle decomposition of a compact n-manifold, then every continuous map $f : M \to X$ is homotopic to a transverse map g. Moreover, if $f\,|_{\partial M}$ is transverse, then there is a homotopy of f rel ∂M to a transverse map.*

Lemma 3.12. *Every cell-complex is homotopy equivalent to a "good" cell-complex.*

For the proof of this lemma, we can apply induction on the i-skeletons and apply Transversality Theorem to the attaching maps.

The purpose of this research is to prove isoperimetric inequalities for certain groups, in other words, we want to compare the volume of n-dimensional balls with the area or volume of their boundary spheres. For this purpose we will be considering handle decompositions of n-balls. The handle decompositions are higher dimensional analogs of van Kampen diagrams. Henceforth, we will denote a handle body diagram or the handle decomposition of a n-ball by (D^n, S^{n-1}) where D^n is an n-ball and S^{n-1} is its boundary sphere .

Example 3.13. Here are a few examples of situations where handle body diagrams are better suited compared to van Kampen diagrams,

1. In case a van Kampen diagram has folded cell pairs. This is illustrated in part (i) of Figure 3.1. However in the same figure part (ii), we have the corresponding part of a handle body diagram and the problem of folding no longer persists.

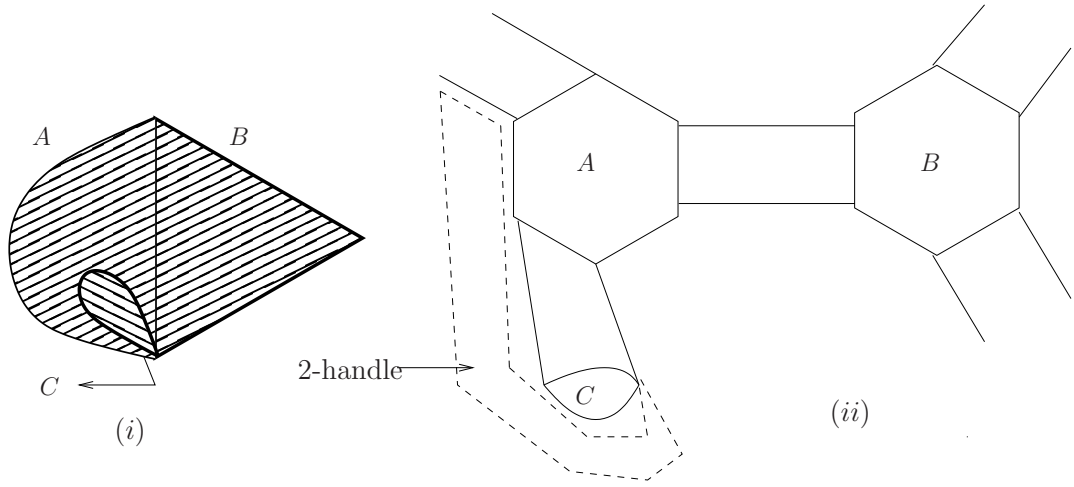

Figure 3.1: (i) Portion of a van Kampen diagram with a folded cell pair, (ii) Corresponding part in a handle body diagram.

2. Another example is shown in part (i) of Figure 3.2 where the 2-cell has been cut open. So, there are seven edges and one face. The corresponding part in a handle body diagram shown in the same figure part (ii), shows a 0-handle with seven 1-handles attached to it in such a way that they correspond to the edges in (i) attached to each other.

Definition 3.14. (*Unreduced Diagram*). A diagram $f : (D^n, S^{n-1}) \to K$ is said to be *unreduced* if in the interior of (D^n, S^{n-1}) there exists two 0-handles H_1^0 and H_2^0 joined together by a 1-handle such that, $f(H_1^0) = f(H_2^0)$ is an open n-cell in

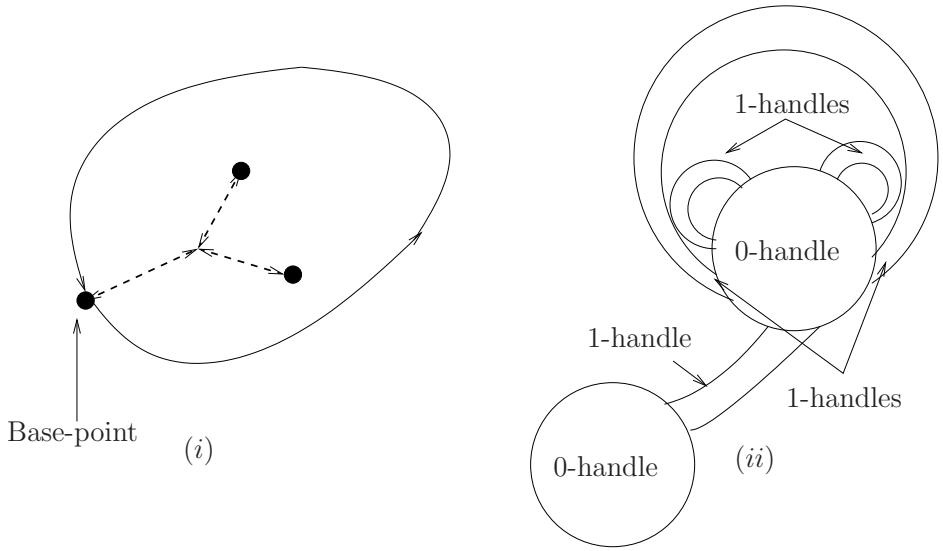

Figure 3.2: (i) Portion of a van Kampen diagram with a 2-cell which has been cut open, (ii) Corresponding part in a handle body diagram.

K and $(f|_{H_1^0}{}^{-1} \circ f|_{H_2^0})$ is an orientation reversing map. Otherwise, the diagram is said to be *reduced*.

In other words, a diagram is *unreduced* if there exists another diagram with the same boundary length or area (in case of 2 or 3-dimensional cases respectively) but strictly smaller filling area or volume for 2 or 3-dimensional cases respectively. Under these circumstances we will eliminate these 0-handles along with the 1-handle connecting them but keeping the boundary of the diagram same and ensuring that we still have a disc. Hence, our intention is to get a *reduced* diagram from an *unreduced* one. We will give an example in a 2-dimensional case via figures and also a method of obtaining a reduced diagram given an unreduced one (Example 3.16). But first here is an example of a handle-body decomposition in 3-dimensions which may or may not be a reduced diagram.

Remark 3.15. Note that all the maps discussed in the rest of this section, from the (reduced or unreduced) diagrams to the ambient space K will be *admissible*

maps (Definition 2.20).

Example 3.16. Given an unreduced diagram $f : (D^2, S^1) \to K$, there is a disc $D^{2\prime}$ such that D^2 and $D^{2\prime}$ have the same boundary but $D^{2\prime}$ has fewer 0-handles. Moreover there is a transverse map $f' : D^{2\prime} \to K$ such that $f|_{\partial D^2} = f'|_{\partial D^{2\prime}}$ and f' is also an admissible map.

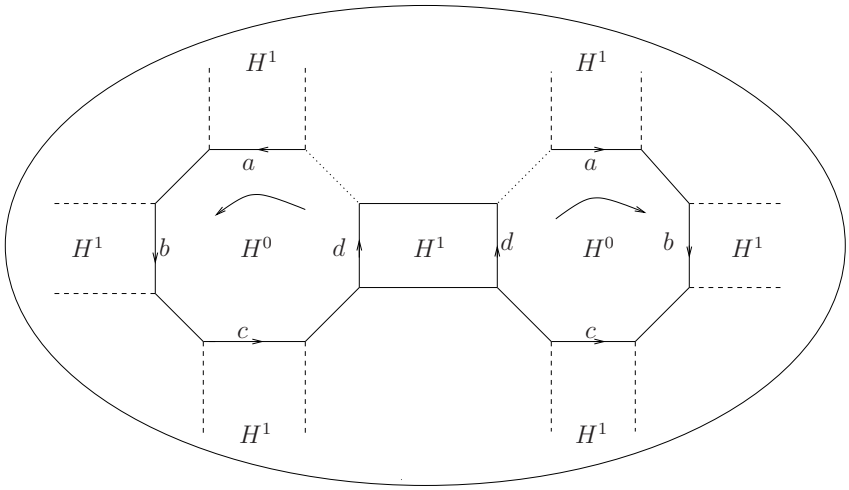

Figure 3.3: Unreduced diagram

In the Figure 3.3, the diagram seen has 0-handles which are 2-discs or blown-up versions of the 2-cells present in the ambient space i.e; if the 2-cells in the original space is an n-gon (n sided polygon), then the corresponding 0-handle will be a $2n$-gon. This diagram is unreduced since there is a pair of 0-handles which have the properties mentioned in Definition 3.14.

Once we remove the pair of 0-handles along with the 1-handle connecting them, we have the annulus $(D^2 \setminus D_1^2) \subset D^2$ be named A^2. The annulus is illustrated in Figure 3.4 below.

Next, we identify the opposite edges, labeled with the same letters a, b, c etc. This is possible as they are mapped to the same edge in K via f. So there is

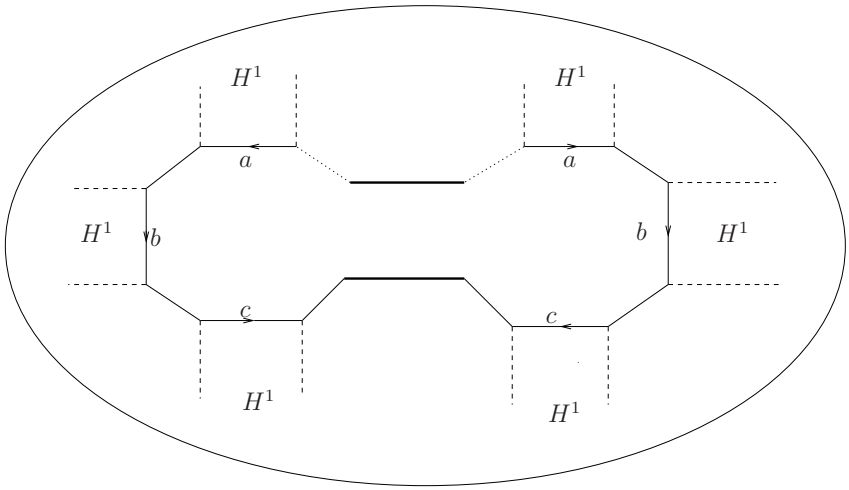

Figure 3.4: Annulus A^2

a homeomorphism α , from one of these edges for example the one named b, to the same edge in K and there is another homeomorphism β from the other edge in the annulus $A^2/_\sim$ labeled b to the same edge in K mentioned above . The composition $(\beta^{-1} \circ \alpha)$ is a homeomorphism between the two edges labeled b in the annulus $A^2/_\sim$. This operation of identifying homeomorphic edges can be denoted by a new equivalence relation $\sim'$. Once all the edges with the same labels are identified with each other we have the following situation (Figure 3.5) but $(A^2/_\sim)/\sim'$ $(= D^{2'})$ is again a disc with the same boundary as the original disc D^2.

Since this does not change the boundary, $f|_{\partial D^2} = f_1|_{\partial D^{2'}}$. If f_1 is not a transverse map then by the Transversality theorem (Theorem 3.11) we have a transverse map f' such that $f' \sim f_1$ and f' has all the same properties as f_1, most importantly, $f|_{\partial D^2} = f'|_{\partial D^{2'}}$.

Next we will discuss how to obtain a reduced diagram from an unreduced one. This argument was given by Brady and Forester ([8]).

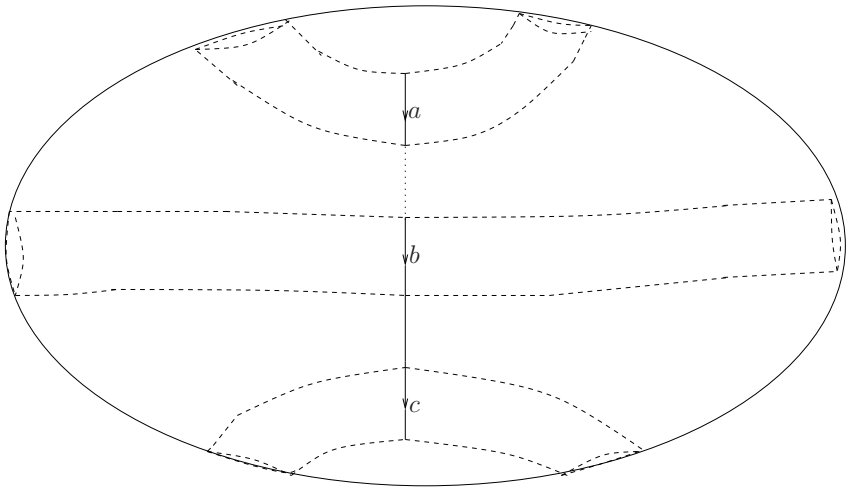

Figure 3.5: Disc $D^{2'}$ (with 1-handles shown in dotted lines)

Let $f : (D^n, S^{n-1}) \to K$ be an admissible map, and let H_1^0 and H_2^0 be 0-handles in (D^n, S^{n-1}) connected together with a 1-handle. Let α be a core curve in the 1-handle connecting H_1^0 and H_2^0 homeomorphic to an interval (Figure 3.6). Suppose f maps α to a point and maps H_1^0 and H_2^0 to the same n-cell, with opposite orientations. As H_1^0 and H_2^0 are 0-handles, there are homeomorphisms $h_i : (H_i^0, \partial H_i^0) \to (D^n, S^{n-1})$ such that $f|_{H_i^0} = \phi \circ h_i$ for some characteristic map $\phi : (D^n, S^{n-1}) \to K$. We first consider the curve α along with a tubular neighborhood around it and collapse it to a point to get part (ii) of Figure 3.6. Next remove the interiors of H_i^0 from (D^n, S^{n-1}) and form a quotient (D_1^n, S_1^{n-1}) by gluing boundaries via $h_0^{-1} \circ h_1$, an orientation reversing map. The new space maps to K by f, and there is a homeomorphism $g : (D^n, S^{n-1}) \to (D_1^n, S_1^{n-1})$. Now $f \circ g$ is an admissible map $(D^n, S^{n-1}) \to K$ with two fewer 0-handles. The map can be then be made transverse with the rest of the 0-handles unchanged. Figure 3.6 illustrates the method pictorially.

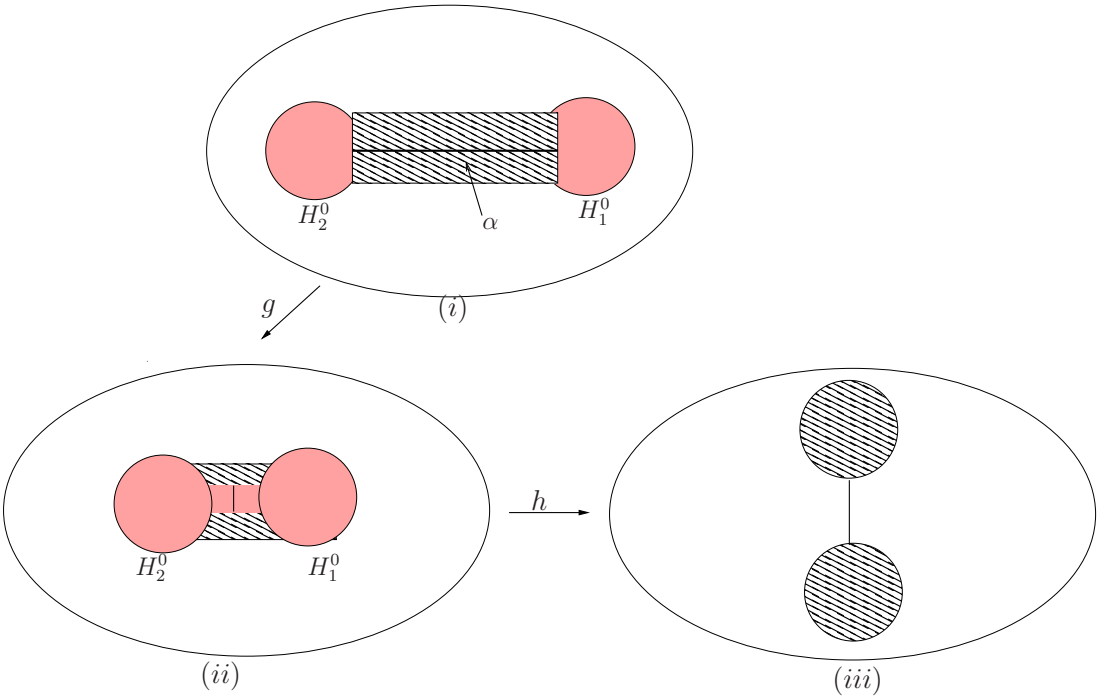

Figure 3.6: (i) two 0-handles joined by a 1-handle and core curve α, (ii) Picture of (i) after α has been removed, and (iii) Final Picture

Chapter 4

Lower Bounds for Nil and Sol

Here we provide lower bounds for second order Dehn functions in case of lattices in the Nil and Sol geometries. The argument used here to obtain these bounds is due to Brady and Forester [8].

4.1 The connection between Linear Algebra and Cell Decomposition of Mapping Tori

In this section we discuss the structure of the 3-dimensional manifolds that have the lattices of the Nil and Sol geometries as fundamental groups.

The 3-manifolds considered here are the mapping tori where the attaching maps corresponds to matrices in $SL_2(\mathbb{Z})$. In other words, given a group of the form $\mathbb{Z}^2 \rtimes_{\psi_A} \mathbb{Z}$, where $\psi_A \in Aut(\mathbb{Z}^2)$ and can be represented by a matrix $A \in SL_2(\mathbb{Z})$, the geometric realization of these groups are mapping tori where the attaching maps are the automorphisms of $\mathbb{Z}^2$. For example if ψ_A is the identity map then, the corresponding space is $\mathbb{Z}^3 \subset \mathbb{R}^3$. Other specific examples we are interested in are the lattices in the 3-dimensional geometries Nil and Sol. In

particular we will be looking at lattices corresponding to the matrix $\begin{pmatrix} 1 & 1 \\ 0 & 1 \end{pmatrix}$ for Nil and $\begin{pmatrix} 2 & 1 \\ 1 & 1 \end{pmatrix}$ in case of Sol. Another way of looking at these are as torus bundles over the circle and they are described below.

Let us denote the mapping torus $\frac{T\times I}{(t,0)\sim(\psi_A(t),1)}$ by A_T, where ψ_A is the attaching map. Let ψ_A be represented by the matrix $A \equiv \begin{pmatrix} x & z \\ y & w \end{pmatrix} \in SL_2(\mathbb{Z})$. So, if the generating curves of the torus in A_T are labeled a, b, then the presentation of the corresponding fundamental group is given by,
$\Gamma = \langle a, b, t \mid [a, b], tat^{-1} = A(a) = a^x b^y,\ tbt^{-1} = A(b) = a^z b^w \rangle$.

4.1.1 Cell Decomposition of the Mapping Torus A_T

We know that the mapping torus A_T consists of two copies of the torus attached via the map ψ_A. Here we will demonstrate an effective way of triangulating the 2-cell spanned by the generators of the group Γ and hence obtain a model space for Γ.

We subdivide the 2-cells of both copies of the torus in A_T into a either a number of triangular faces or a combination of triangular and quadrilateral faces. The following example illustrates this process in details.

Example 4.1. Let $A \equiv \begin{pmatrix} 1 & 1 \\ 0 & 1 \end{pmatrix}$, then the corresponding group is the 3-dimensional, integral Heisenberg group $\mathcal{H} = \langle a, b, t \mid [a, b],\ tat^{-1} = a,\ tbt^{-1} = ab \rangle$.

This subdivision of the mapping tori below, (Figure 4.2) shows that the top

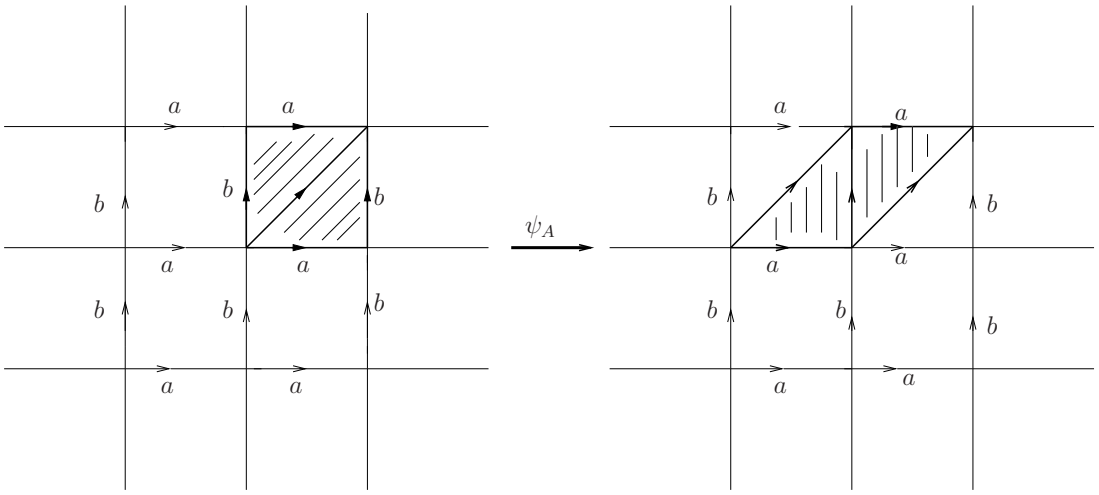

Figure 4.1: Sub-division of $\mathbb{R}^2$ under the action of the map ψ_A .

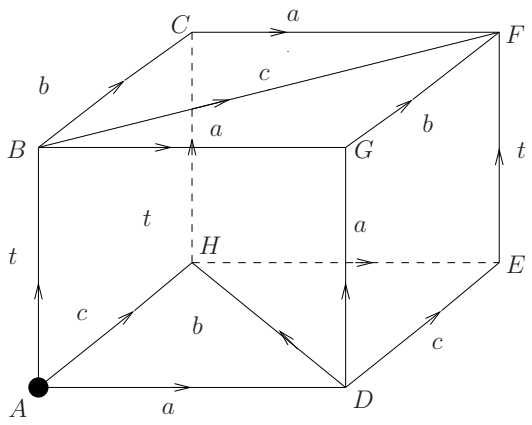

Figure 4.2: The mapping torus corresponding to the matrix A above.

has been divided into two triangular faces each of which can be mapped via ψ_A to their exact replicas in base. This is the picture of the model space for the group $\mathcal{H}$ which is piecewise Riemannian. This 3-cell also serves as the fundamental domain for the action of $\mathcal{H}$ on the corresponding universal cover. The base point is named A and all other vertices of the cell are also labeled.

Example 4.2. If we have the matrix $B \equiv \begin{pmatrix} 2 & 1 \\ 1 & 1 \end{pmatrix}$, then the corresponding group presentation is $\mathcal{S} = \langle a, b, t \ \mid \ [a, b],\ tat^{-1} = a^2b,\ tbt^{-1} = ab \rangle$.

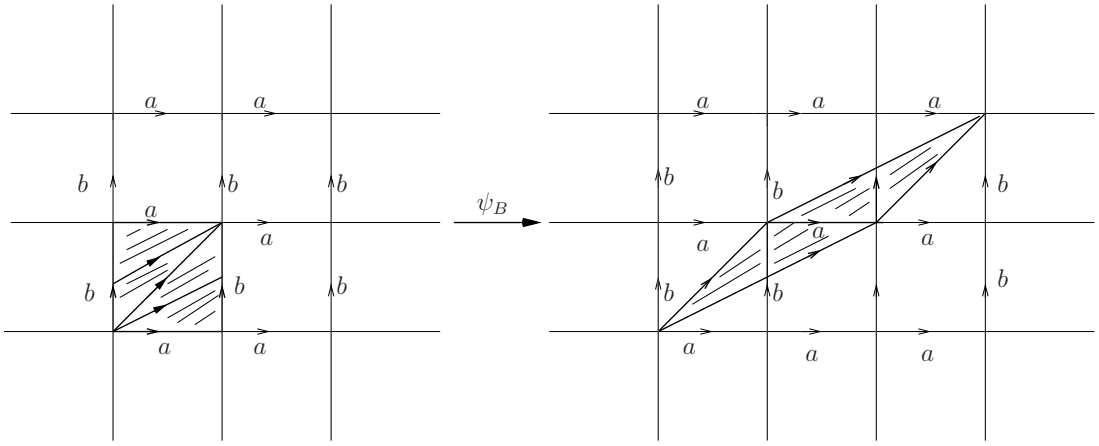

Figure 4.3: Sub-division of two copies of $\mathbb{R}^2$ under the action of ψ_B .

Again Figure above shows that the subdivision is compatible to the relations in the group presentation $\mathcal{S}$.

This triangulation of the mapping tori below, (Figure 4.4) shows that the top has been divided into four triangular faces each of which can be mapped via ψ_B to their exact replicas in base. This is the picture of the model space for the group $\mathcal{S}$ which is piecewise Riemannian. This 3-cell also serves as the fundamental domain for the action of $\mathcal{S}$ on the corresponding universal cover.

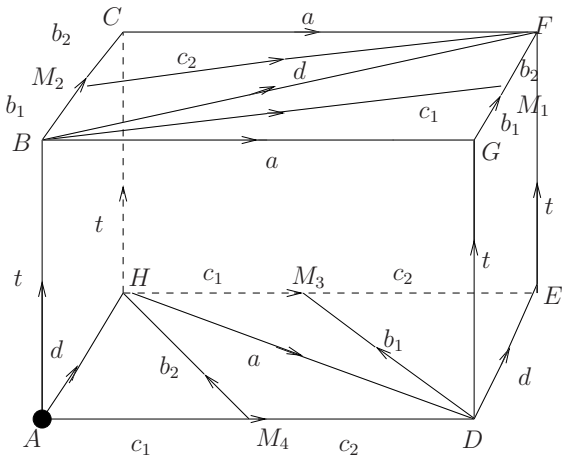

Figure 4.4: The mapping torus corresponding to the matrix B above.

4.2 The Lower Bounds

In this section provide lower bounds for the second order Dehn function for $\mathcal{H}$ and $\mathcal{S}$ and show that the growth of balls in the first case is polynomial while in case of the latter it is exponential.

Let M be the 3-manifold corresponding to the lattice $\mathcal{S}$ in the Sol geometry mentioned above in Example 4.2 (along with the triangulation shown). Let $\widetilde{X}$ be its universal cover. So, one can find numerous copies of M inside $\widetilde{X}$. To obtain a lower bound for the second order Dehn function in case of the lattice of the Sol geometry, we will exhibit a sequence of embedded balls $B_n \subset \widetilde{X}$. This argument is due to Brady and Forester [8].

We will construct a ball in $\widetilde{X}$, by defining regions $R_n \subset M$ which are easy to measure in the Riemannian metric. Then we approximate these regions using combinatorial subcomplexes in $\widetilde{X}$.

Notation 4.3. In this section we will denote the volume of an 3-ball by $Vol^3(B^3)$ and the area of its boundary sphere by $Area(S^2)$.

The matrix $\begin{pmatrix} 2 & 1 \\ 1 & 1 \end{pmatrix}$ has two eigenvalues $\lambda > 1$ and $\mu < 1$. Now let us define in the coordinates of M, $R_n = [0, \lambda^n] \times [0, 1] \times [0, n]$, Figure 4.5.

The volume of R_n can be easily computed by integration. The area of a horizontal slice $A = [0, \lambda^n] \times [0, 1] \times z$ is λ^n so area of R_n is given by $6\lambda^n$, integration in the z-coordinate gives us $Vol(R_n) = n\lambda^n$.

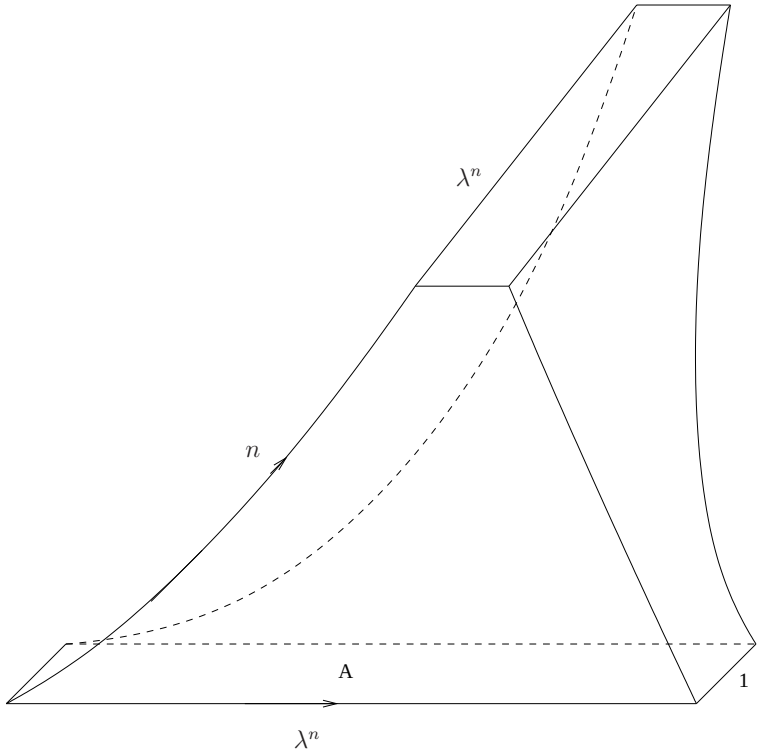

Figure 4.5: Region R_n in case of Sol.

Then we approximate the Riemannian regions using combinatorial subcomplexes which are described briefly below. Let $S_{i,n} \subset \mathbb{R}^2 \times [i-1, i]$ for $1 \leq i \leq n$ be subcomplexes in $\widetilde{X}$ such that $R_n \subset S_n = \bigcup_{i=1}^{n} S_{i,n} \subset R'_{n+k}$, where R'_{n+k} is a translate of $R_{n+k}, k > 0$ in the x and y-directions. The details of the construction of the subcomplexes S_n^i can be found in Section 4 of [8].

Therefore the ball obtained after the approximation in the step above, has volume $\geq n\lambda^n \approx Area(\ln(Area))$.

Remark 4.4. The lower bound argument with all necessary details can be found in the paper by Brady and Forester, [8].

Lemma 4.5. *If $B(n)$ is a ball of radius n in $\widetilde{X}$ corresponding to $\mathcal{S}$, then $|B(n)| \sim \mathcal{O}(k^n)$, for some positive constant k.*

Proof. In order to determine the lower bound of the growth of balls in the case of the group $\mathcal{S}$, we will show that the monoid generated by $\langle t, ta\rangle$ is a free group embedded in the group $\mathcal{S}$.

Let us denote the matrix $\begin{pmatrix} 2 & 1 \\ 1 & 1 \end{pmatrix}$ associated with this group by M. In the vector notation we write t as the zero vector $\overrightarrow{0}$ and ta as the vector $\overrightarrow{a}$. The following is a list of elements, at level two we have four elements, $t^2, tta, tat, tata$ which may be represented in vector notation as $\overrightarrow{0}, \overrightarrow{a}, M^{-1}\overrightarrow{a}, \overrightarrow{a}+M^{-1}\overrightarrow{a}$ respectively. Similarly in level three we have $t^3, t^2ta, ttat, tat^2, ttata, tatta, tatat, tatata$ represented by $\overrightarrow{0}, \overrightarrow{a}, M^{-1}\overrightarrow{a}, M^{-2}\overrightarrow{a}, \vec{a}+M^{-1}\vec{a}, \vec{a}+M^{-2}\vec{a}, M^{-1}\vec{a}+M^{-2}\vec{a}$, $\vec{a}+M^{-1}\vec{a}+M^{-2}\vec{a}$ respectively. So in general, at each level $i, i \geq 1$ we have 2^i elements and in the general case, ignoring the negative power of M, the elements have the form $\vec{a}, M\vec{a}, M^2\vec{a}, ..., M^i\vec{a}, \vec{a}+M\vec{a}, \vec{a}+M^2\vec{a}, ..., \vec{a}+M^i\vec{a}$ etc. Next we claim that each of these vectors are distinct. In fact, at each stage the vectors get stretched by a factor of $\lambda > 1$, one of the eigenvalues of the matrix M (Figure 4.6). For a large positive integer N the stretching factor is λ^N. For instance, it is easy to see $M\vec{a}, M^2\vec{a}$ are each different from $\vec{a}$ and $M\vec{a}+M^2\vec{a}$ is different from $\vec{a}$ and so on.

Now if we proceed by induction on the number N. For $N = 1$, it is easy to

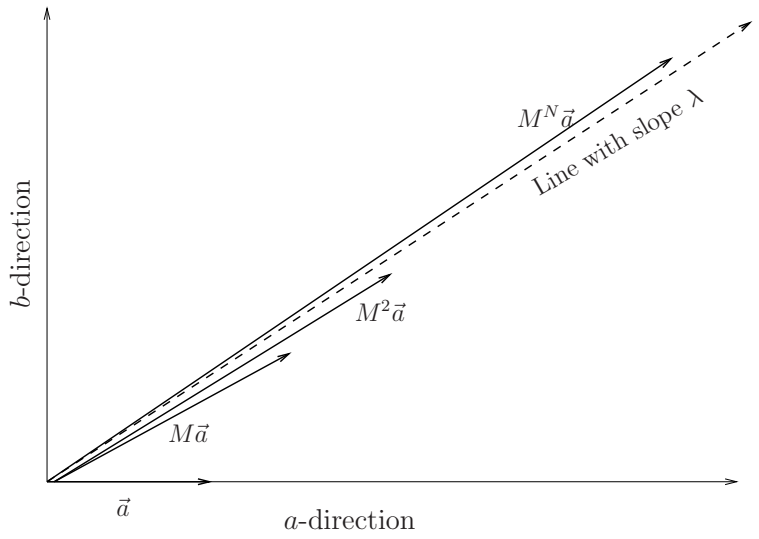

Figure 4.6: Stretching the vectors.

see that the vectors given above are all distinct. Let us consider this to be true for some specific N, this is the induction hypothesis. If we project these vectors on to the plane it looks like the following Figure 4.7, which gives an idea of the geometric growth.

At the $N+1$ level we see the part marked Z, after the vertex marked λ^{N+1} is distinct by the induction hypothesis and the remaining portion starting at the end of X is distinct as it consists of vectors of the form $M^{N+1}\vec{a}, M\vec{a} + M^{N+1}\vec{a}, ..., M^N\vec{a} + M^{N+1}\vec{a}$ which are stretched more than $M^N\vec{a}$ but less than $M^{N+1}\vec{a}$.

Therefore we have a free group inside which means that the growth of the balls (of radius n) in the manifold corresponding to $\mathcal{S}$ is bounded below by λ^N.

The upper bound for the cardinality is same as the upper bound on cardinality of balls corresponding to a free group on three generators. So at level k in Figure 4.8 we have at most 6.5^k elements. Therefore a ball of radius n has at most $\sum_{k=0}^{n} 6.5^k + 1$ elements. So, $|B(n)| \leq \frac{3}{2}(5^n) - \frac{1}{2} < Const.5^n$.

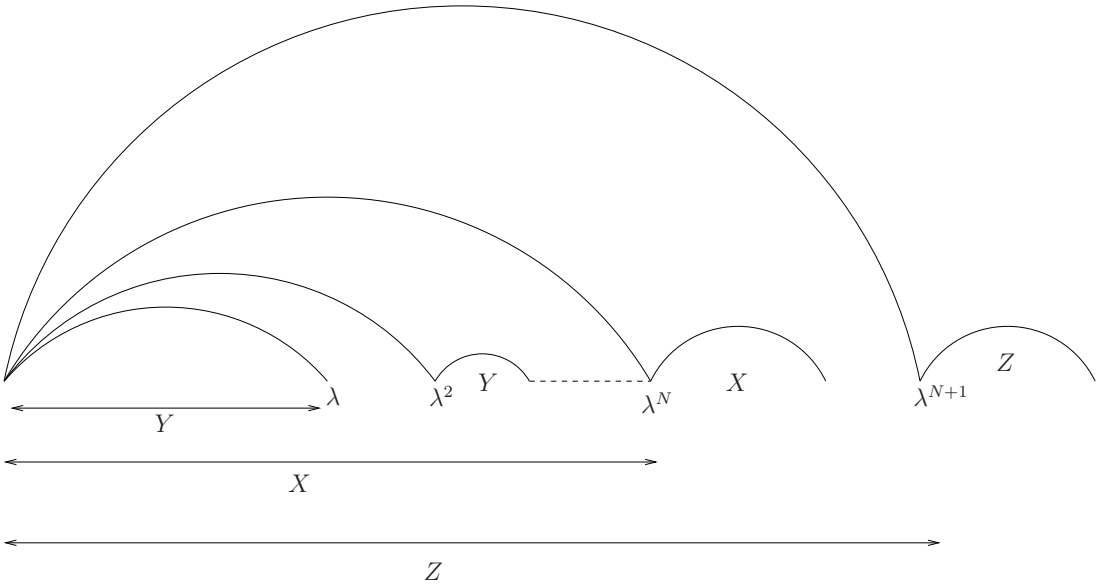

Figure 4.7: Projection of the vectors in the plane.

So $|B(n)| \sim \mathcal{O}(k^n)$ for a positive constant k, where $\lambda \leq k \leq 5$.

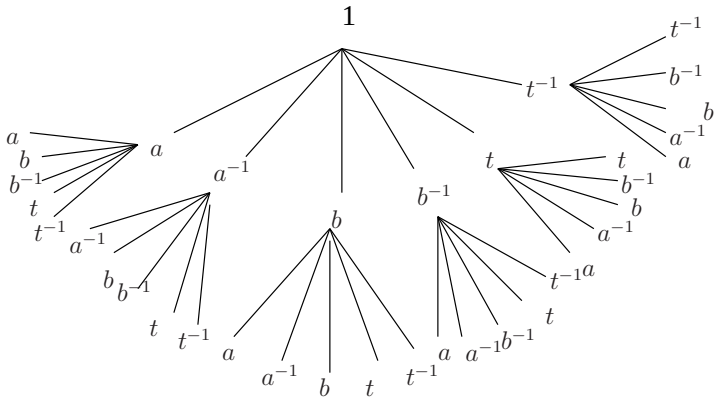

Figure 4.8: Number of elements in a ball of radius 1, 2 etc.

□

Proposition 4.6. *Given an embedded 3-ball B^3,with boundary sphere S^2 in the universal cover corresponding to $\mathcal{H}$, $Vol^3(B^3) \succeq (Area(S^2))^{\frac{4}{3}}$.*

Proof. In order to show this we will exhibit a sequence of embedded balls $B_n \subset \widetilde{X}$.

(This argument is due to Brady and Forester [8]). We will construct a ball in $\widetilde{X}$, by defining regions $R_n \subset X$ which are easy to measure in the Riemannian metric. Then we approximate these regions using combinatorial subcomplexes in $\widetilde{X}$.

Let us consider R_n to be the region $[0, n^2] \times [0, n] \times [0, n]$. Then approximate this Riemannian region combinatorially by filling it with 3-cells in the universal cover of the complex associated with $\mathcal{H}$ and each of the 3-cells have the appropriate cell decomposition shown in Example 4.2.

Consider the following figure (Figure 4.11) which partially shows how to build a 3-ball that fills a given 2-sphere in case of Nil. At level (1) we see that the base is a parallelogram with a and c sides so we extend the base on either side by adding triangular regions of length to obtain a square base with sides a and b. The extra area added on each side is $\frac{1}{2}n^2$. We go on in this way until we reach the nth level, adding areas at each level exactly equal to n^2, the extra area added after level (2) is $2n^2$. So total area of the faces at the front and back add up in the following way $n+2n+3n+.....+n^2 = n\left(n(\frac{n+1}{2})\right) \sim \mathcal{O}(n^3)$. Area of the faces on the sides add up to give, $2n^3 + n^2(n-1)$ while the area of the top is n^2 and the base after n levels is $\sim \mathcal{O}(n^3)$. The area of all faces of the ball is $(Area_{Top} =)n^2 + (Area_{Sides}) = (3n^3 - n^2) + (Area_{Front+Back} =)(n^3 + n^2) + (Area_{Base} =)n^3$ Thus the total area is $Area(S^2) = 5n^3 + n^2$ and for a large value of n, $(n \geq 1)$, $Area \leq const.n^3 \preceq \mathcal{O}(n^3)$. The volume of this ball is therefore $\geq \mathcal{O}(n^4)$.

Next we claim that this ball is an optimal filling of the sphere S^2 because if there was one other ball filling it along with the one constructed above, then this would give rise to a non-trivial 3-cycle in a contractible 3-complex which is a contradiction. In other words, we would see a 3-sphere sitting inside a contractible 3-complex. So in conclusion we can say that $Vol^3(B^3) \succeq (Area(S^2))^{\frac{4}{3}}$.

□

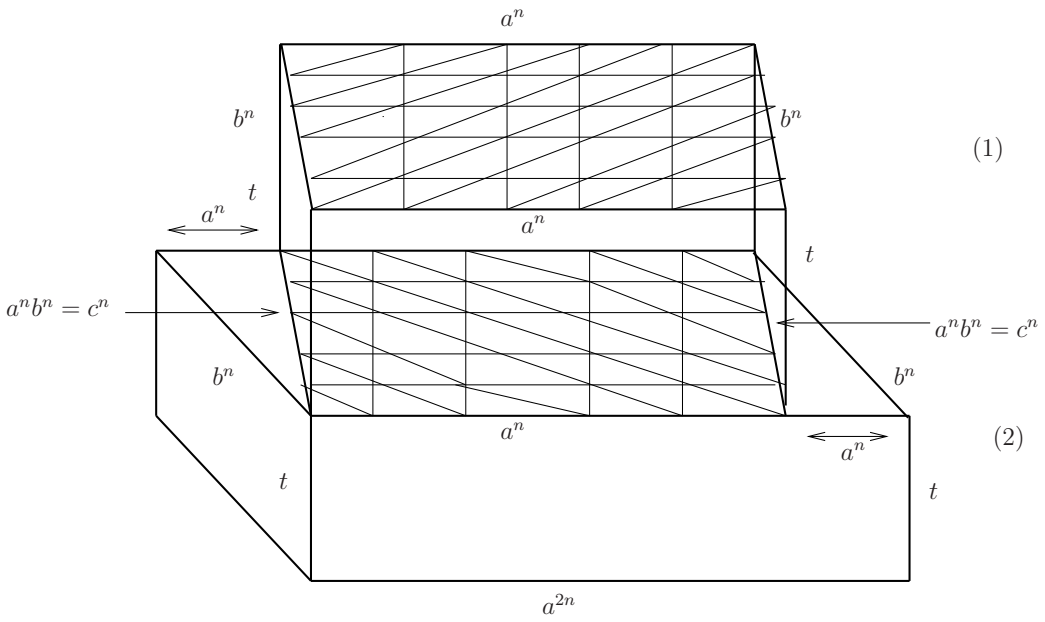

Figure 4.9: First two layers of optimal ball filling of a 2-sphere.

Remark 4.7. From the previous proposition we obtain a lower bound for the second order Dehn function for $\mathcal{H}$, $\delta^{(2)}(n) \succeq n^{\frac{4}{3}}$.

Lemma 4.8. *If $B(n)$ is a ball of radius n in case of $\mathcal{H}$, then $|B(n)| \sim \mathcal{O}(n^4)$.*

Proof. Let us start by considering the brick shown in the following picture (Figure 4.2). The structure of the brick is same as the ball shown in the proof above (Figure 4.11). In order to obtain a lower bound for the growth of balls in this case we will show that any vertex in this ball is in a ball of radius $4n$ and that the number of elements in the brick is $\sim \mathcal{O}(n^4)$.

Let us look at the Figure below where we have a clear picture of the top and base of the subcomplexes in the ball at each level. Let A denote the base point now, if we consider any point in the face F_1 can be reached via a path of length $\leq n$. The point C which is farthest from A but the length of the path is n.

Next let us consider the second level (2), any point in F_2 can be reached via

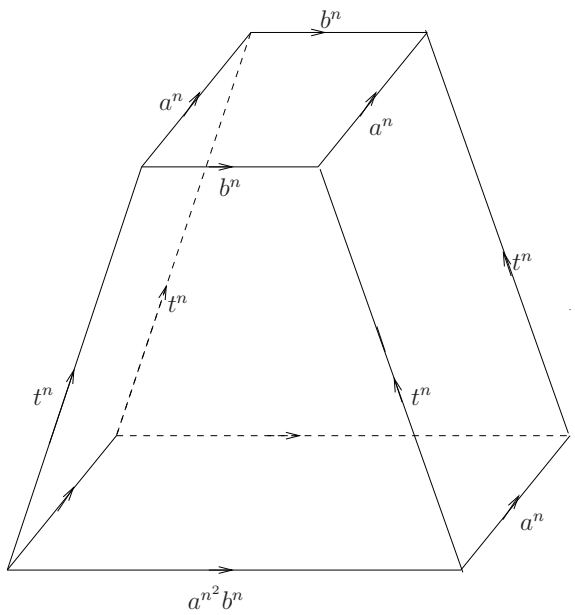

Figure 4.10: The ball $B_i(n)$ in the Cayley graph corresponding to $\mathcal{H}$ above.

a path of length $\leq (n+1)$, any point the left triangular face can be reached via a path of length $\leq (n+1)$. On the other hand the points on the right hand triangular face can be reached via a path of length $\leq (2n+1)$. The length of the path from the base point to C_1 is exactly $(n+1)$.

Proceeding in the same way, we look at level (3) and there is a path of length $\leq (2n+2)$ from A to any point in F_3. Length of path from the base point to C_2 is again $\leq (2n+2)$. In general, at level (i), $1 \leq i \leq n$, the length of a path from A to any point in F_i or the triangular faces on both sides is $\leq (2n+i)$.

Therefore after n levels the lengths of paths from A to any point in F_n is at most $3n$. So, this brick is in a ball of radius at least $3n$.

Now the number of elements in level (1) is n^2, level (2) is $(2n)n$. In general at any level $(i), 1 \leq i \leq n$, the number of elements is $(in)n$. Hence the total number of elements in the brick is $n^2(1+2+....+n) = n^2\left(\frac{n(n+1)}{2}\right) \sim \mathcal{O}(n^4)$.

Next for an upper bound, we have the following lemma,

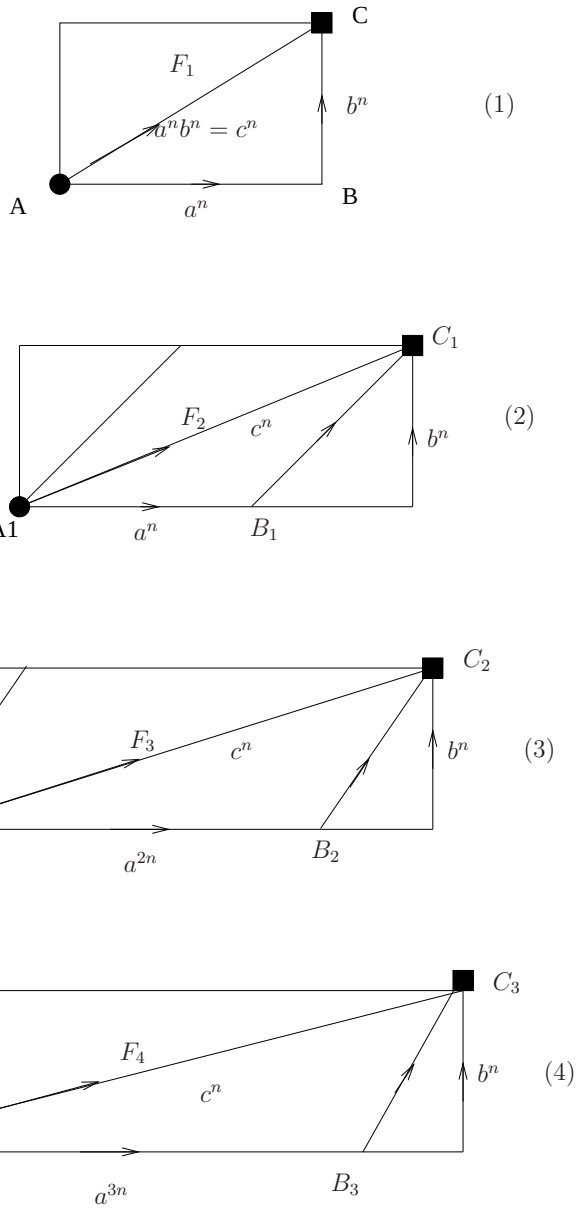

Figure 4.11: First two layers of optimal ball filling of a 2-sphere.

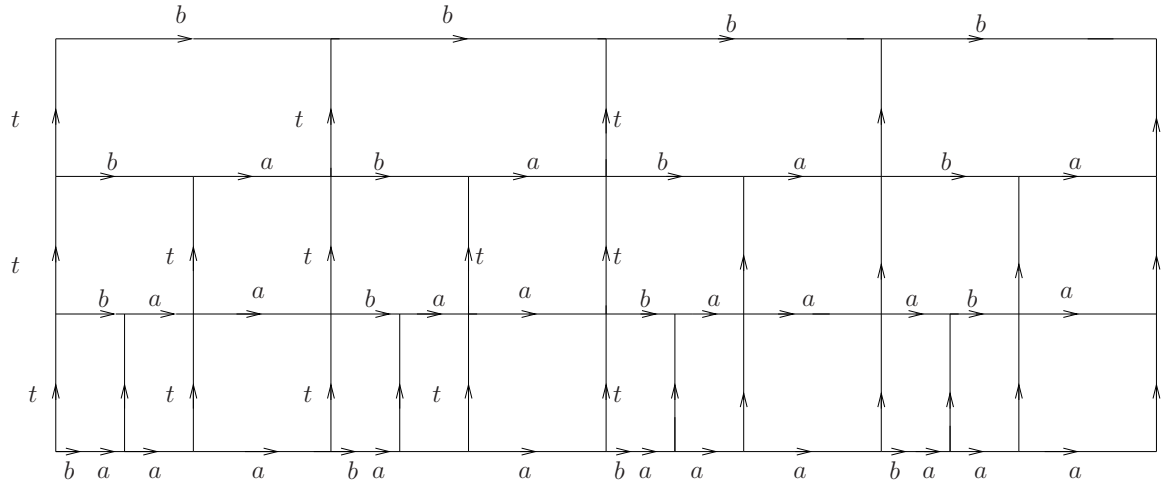

Figure 4.12: Face (F_1) of $B_i(r)$ in the Cayley graph of $\mathcal{H}$.

Lemma 4.9. *Any word w in $\mathcal{H}$ in the letters $a^{\pm 1}, b^{\pm 1}$ and $t^{\pm 1}$ where, $|w| \leq r$ can be reduced to its normal form $a^x b^y t^z$ such that $|x| \leq n^2, |y| \leq n$ and $|z| \leq n$.*

Proof. We should note that if we have the following subwords in w, they can be replaced with those mentioned alongside,
$ta = at, tb = abt, tb^{-1} = b^{-1}t, ta^{-1} = a^{-1}t, t^{-1}b = a^{-1}bt^{-1}, t^{-1}b^{-1} = ab^{-1}t^{-1}, t^{-1}a = at^{-1}, t^{-1}a^{-1} = a^{-1}t^{-1}$.

We will start by moving all the occurrences of t or t^{-1} in w to the right using the relations shown above and it is clear from these relations that the number of t, t^{-1} do not increase in the process. So now we have a word of the form $a^x b^y t^z$, where $|z| \leq n$, also note the number of b, b^{-1} remain the same but the number of a or a^{-1}, increases, in fact for each instance of b or b^{-1} we end up with an extra a or a^{-1} hence, we end up with at most product of number of t, t^{-1} and the number of b, b^{-1} both of which are bounded above by n, so we have $|x| \leq n^2$.

□

Recall that the ball of radius n for a finite presentation $\mathcal{P} = \langle \mathcal{A} \mid \mathcal{R} \rangle$ is defined

by $B(n) = \{w \in \mathcal{F}(\mathcal{A}) : |w| \leq n\}$. Therefore the total number of words possible in a ball of radius r is $\leq n^4$. $\square$

Chapter 5

Upper Bounds- Reduction to Varopoulos Isoperimetric Inequality

Chapters 5 and 6 are devoted to obtaining upper bounds for the second order Dehn functions of $\mathcal{H}$ and $\mathcal{S}$ using a variation of Varopoulos Transport argument.

In chapter 5 we reduce the original isoperimetric problem involving volume of 3-balls and areas of their boundary 2-spheres to a problem involving Varopoulos' notion of volume and boundary of finite domains in dual graphs.

5.1 Definitions

Since we will use barycentric subdivisions to obtain the dual graph, we will start this chapter with the following definitions. (These definitions and notations have been taken from[13].)

Definition 5.1. (*Barycentric Subdivision of a convex polyhedral cell*) Let C be

a polyhedral cell in an n-dimensional polyhedral complex K. The barycentric subdivision of C denoted by C' is the simplicial complex defined as follows: There is one geodesic simplex in C' corresponding to each strictly ascending sequence of faces $F_0 \subset F_1 \subset .... \subset F_n$ of C; the simplex is the convex hull of barycenters of F_i. Note that the intersection in C of two such simplices is again such a simplex. The natural map from the disjoint union of these geodesic simplices to C imposes on C the structure of a simplicial complex - this is C'.

Definition 5.2. (*Barycentric Subdivision of a polyhedral n-complex K*) Let $p : \coprod_\lambda C_\lambda \to K$ (where C_λ are the polyhedral cells of K), be a projection. For each cell C_λ we index the simplices of the barycentric subdivision C'_λ by a set I_λ; so C'_λ is the simplicial complex associated to $\coprod_{I_\lambda} S_i \to C_\lambda$ where S_i denotes the simplices of C'_λ. Let $\lambda' = \coprod_\lambda I_\lambda$. By composing the natural maps $\coprod_{I_\lambda} S_i \to C_\lambda$ and $p : \coprod_\lambda C_\lambda \to K$ we get a projection $p' : \coprod_{i\in\lambda'} S_i \to K$. Let K' be the quotient of $\coprod_{i\in\lambda'} S_i$ by the equivalence relation $[x \sim y$ iff $p'(x) = p'(y)]$. K' is the barycentric subdivision of K.

Note 5.3. : Given any complex, there is a poset $\mathcal{P}$ on the cells of the complex ordered by inclusion. Therefore for any ascending chain in $\mathcal{P}$ there is a simplex in the barycentric subdivision of the complex.

5.2 Dual Graphs

The examples in the previous section gives us an idea of the cell decomposition of the spaces under consideration. The groups considered here are all finitely generated, so the groups act properly and cocompactly by isometries on their respective universal covers. In fact, the translates of the fundamental domain covers the universal cover $\widetilde{X}$ in each case.

It is essential to mention here that the only groups we are interested in are the 3-dimensional groups $\mathcal{H}$ and $\mathcal{S}$ from Section 4.1 and we will use the letter G to refer to them in general.

Next, we define the dual graph Γ using Definition 5.8. The vertex set of Γ, $V_\Gamma = \{\sigma : \sigma \text{ is a 3-cell of } \widetilde{X}\}$ while the edge set is, $E_\Gamma = \{\tau : \tau$ is a codimension one face (2-cells) shared by two adjacent 3-cells of $K\}$.

Lemma 5.4. *There is a map that embeds the graph* Γ *in* K.

Proof. Consider the barycentric subdivision of both the graph Γ and the universal cover $\widetilde{X}$, we denote these barycentric subdivisions by Γ' and $\widetilde{X'}$ respectively. Next we map the vertices in V_Γ to the barycenters of the 3-cells while we map the barycenter of an edge τ, labeled by τ_m in E_Γ to the barycenter of the codimension one face shared by the two 3-cells in V_Γ, serving as the initial and terminal vertices of τ. Finally, if τ is an edge with initial and terminal vertices σ_1 and σ_2 respectively, then, the left half-edge of τ is mapped to the simplex in K' corresponding to the ascending chain $\tau \subset \sigma_1$ in the poset $\mathcal{P}$ while, the right half-edge maps to the simplex in K' corresponding to the ascending chain $\tau \subset \sigma_2$ in $\mathcal{P}$.

As there is a natural bijection between the barycentric subdivision of a space and the geometric realization of the space itself so, there is a map which takes Γ into K. □

So, now we have a dual graph in $\widetilde{X}$ which is also a Cayley graph (with the same name Γ), with respect to a finite generating set which we will define subsequently. The aim of the remaining part of this section is to show that Γ is quasi-isometric to $\widetilde{X}$ using $\check{S}varc - Milnor$ Lemma ([13]).

Given a length space X. If a group G acts properly and cocompactly by isometries on X, then G is finitely generated and for any choice of basepoint $x_0 \in X$, the map $f : G \to X$, defined by $g \mapsto g.x_0$ is a quasi-isometry.

Let C be the fundamental domain of $\widetilde{X}$ (a compact subset of $\widetilde{X}$ such that its translates covers all of $\widetilde{X}$). We then define the generating set of the group G in the following way, $\mathcal{A} = \{g \in G \mid gC \cap C = codimension - one\ face\}$.

In case of $\mathcal{H}$ the valence of a vertex is eight, while in the case of $\mathcal{S}$ the valence is twelve. Hence, the generating sets in these cases will contain four and six elements respectively. We will define the generating sets in detail for specific examples i.e, for the groups $\mathcal{H}$ and $\mathcal{S}$ in the following lemma.

Note 5.5. In the following lemma, we shall denote the triangular faces of the cell decomposition obtained in the previous section as $\triangle XYZ$, where X, Y, Z are the labels of vertices in the cell decomposition forming a triangle.

Lemma 5.6. *Given the cell decompositions for groups $\mathcal{H}$ and $\mathcal{S}$ in section 4.1:*

1. *$\mathcal{A}_0 = \{b, c, t, tb\}$ is a finite generating set for $\mathcal{H}$, where $c = b^{-1}a$ (from Figure 4.2).*

2. *$\mathcal{A}_0 = \{d, t, c_1c_2, td^{-1}, tc_2^{-1}c_1^{-1}, tb_1c_1^{-1}\}$ is a finite generating set for $\mathcal{S}$, where, $a_1a_2 = a, d = ba = ab, c_1 = ab_1, c_2 = b_2a$ (from Figure 4.4).*

Proof. (*of* (i)) We consider Figure 4.2 for this part of the proof. The vertex A is chosen as the base point of universal cover $\widetilde{X}$. Therefore this point represents the identity element of the group. The paths that take the base point to its images in copies of the fundamental domain (which are 3-cells sharing codimension one faces with the fundamental domain) represent the isometries that take the domain to its copies and hence they are the generators of the group with respect to the Cayley

graph Γ. In case of $\mathcal{H}$, there are eight other 3-cells sharing codimension one faces with the fundamental domain or in other words, due to the cell decomposition shown in section 4.1, any 3-cell in the universal cover shares a codimension one face with eight other 3-cells.

In the following lines we give a list of isometries and hence the words which generate translates of the fundamental domain that share a codimension one face with the domain.

The path from A to D represents the isometry b taking the domain to the 3-cell to its right; path from A to H represents the word c takes the domain to the cell behind itself; A to B, the word t takes the domain to the 3-cell on the face $\triangle BCG$; path from A to G, the word tb takes the domain to the 3-cell on the face $\triangle GFC$. The isometries that take the domain to the rest of the neighboring 3-cells, are inverses of the words already mentioned above. For example the isometry taking the domain to the 3-cell sharing the face $\triangle ADE$ is t^{-1}, while the one taking it to the 3-cell associated with the face $\triangle AHE$ is $b^{-1}t^{-1}$ etc. So it is clear that $\mathcal{A}_0 = \{b, c, t, tb\}$ is a finite generating set for $\mathcal{H}$ and ${\mathcal{A}_0}^{-1} = \{b^{-1}, c^{-1}, t^{-1}, b^{-1}t^{-1}\}$.

(*Proof. of* (ii)) This can be shown in a similar way as above. In this case, the fundamental domain shares codimension one faces with twelve other 3-cells, (four cells each above and below, two on each side and the remaining two at the front and back). As before the translates d and t generate copies to the right and vertically above (and sharing the face $\triangle BFM_1$) the fundamental domain respectively. The translate td^{-1} generates the copy sharing the face $\triangle BGM_1$, while $tc_2^{-1}c_1^{-1}$ generates the copy of the fundamental domain along the face $\triangle BM_2F$. Finally $tb_1c_1^{-1}$ is responsible for the copy of the domain sharing the face $\triangle M_2CF$ with the fundamental domain. So $\mathcal{A}_0 = \{d, t, c_1c_2, td^{-1}, tc_2^{-1}c_1^{-1}, tb_1c_1^{-1}\}$. Also, it

is easy to check that ${\mathcal{A}_0}^{-1} = \{d^{-1}, t^{-1}, dt^{-1}, c_1c_2t^{-1}, c_1b_1^{-1}t^{-1}\}$. □

Proposition 5.7. *Cay(G, $\mathcal{A}_0$), the Cayley graph of the group G with respect to the generating sets $\mathcal{A}_0$ defined in Lemma 5.6 is quasi-isometric to $\widetilde{X}$.*

Proof. Milnor's Lemma says that the group G is finitely generated and quasi-isometric to the ambient space $\widetilde{X}$. But the Cayley graph $\mathrm{Cay}(G, \mathcal{A})$ with respect to any finite generating set $\mathcal{A}$ of the group G, is quasi-isometric to the group itself, this quasi-isometry can be seen as the natural inclusion $G \hookrightarrow Cay(G, \mathcal{A})$, defined by $g \mapsto g.1$ for all $g \in G$. This last quasi-isometry is also a simple illustration of Milnor's Lemma.

Finally, two Cayley graphs associated to the same group but with different generating sets are quasi-isometric, this implies $\mathrm{Cay}(G, \mathcal{A}_0)$ is quasi-isometric to $\widetilde{X}$. □

5.2.1 Definitions and Notations

We start with the definition of a dual graph (Section 5.2).

Definition 5.8. Given an ambient n-dimensional space K, we define a graph Γ in the following way:

Vertex set V_Γ: $V_\Gamma = \{\sigma : \sigma$ is a n-cell of $K\}$

Edge set E_Γ: $E_\Gamma = \{\tau : \tau$ is a $(n-1)$-cell and τ is a face of exactly 2 n-cells of $K\}$.

Given a finitely presented group G, let X be the corresponding n-dimensional cell-complex and let $\widetilde{X}$ be its universal cover. Let $f : (D^n, S^{n-1}) \to \widetilde{X}$ be a reduced diagram (defined in Section 3.2) where D^n and its boundary sphere S^{n-1} are either embedded or immersed in $\widetilde{X}$. Note that the map f considered here

is transverse and hence admissible, so each i-handle in the diagram maps to an $(n-i)$-cell in $\widetilde{X}$. Now we have the following definitions.

Definition 5.9. Define a finite subset D of the vertex V_Γ such that,
$D \ = \ \{\sigma : \sigma$ is an n-cell in $\widetilde{X}$ such that $\sigma \in Im(f)\}$.
Associated with D is a function analogous to a characteristic map, given by,
$\phi_D : V_\Gamma \to \mathbb{N} \cup \{0\}$ defined by, $\phi_D(\sigma) =$ number of pre-images of σ under f.

Remark 5.10. Let $||\phi_D|| = \sum_{\sigma \in D} \phi_D(\sigma)$, this is the number of 0-handles in the diagram i.e, $||\phi_D|| = Vol^n(D^n)$ where $Vol^n(D^n)$ denotes the volume of the n-ball D^n.

Remark 5.11. It is clear that if f is an embedding in the above definition then ϕ_D is in fact the characteristic function of the set D.

Next we define the boundary of the finite set D defined above:

Definition 5.12. (*Varopoulos Boundary of D*) is defined to be the set of all $(n-1)$-cells $\tau \in E_\Gamma$ such that τ is a face of exactly two n-cells $\sigma_i, \sigma_j \in V_\Gamma$ such that $\phi_D(\sigma_i) \neq \phi_D(\sigma_j)$, $\partial_V D = \{\tau : \tau \in E_\Gamma$ is a face of two n-cells, $\sigma_i, \sigma_j; \phi_D(\sigma_i) \neq \phi_D(\sigma_j)\}$.

Next we define $\nabla\phi_D : E_\Gamma \to \mathbb{N} \cup \{0\}$ by, $\nabla\phi_D(\tau) = |\phi_D(t(\tau)) - \phi_D(i(\tau))|$, where i and t have the same definition as before.
The cardinality of the Varopoulos boundary $|\partial_V D|$, in this case can be given by,
$\| \nabla\phi_D \| = \sum_{\tau \in \partial_V D} |\phi_D(t(\tau)) - \phi_D(i(\tau))|$.
This definition says that $\tau \in E_\Gamma$ is a boundary edge of D if $\phi_D(t(\tau)) \neq \phi_D(i(\tau))$.

5.2.2 Reducing to Varopoulos Isoperimetric Inequality

In this section we show that our problem to obtain an upper bound for the second order Dehn functions can be reduced to finding an inequality between volume and boundary notions according to Varopoulos in case of $\mathcal{H}$ and $\mathcal{S}$. We start with the following lemma which works in general for dimensions 1 or more.

Lemma 5.13. *$\| \nabla\phi_D \| \leq |\partial D^n|$, where $|\partial D^n|$ is the area or volume of the boundary sphere of the diagram (D^n, S^{n-1}) for $n > 1$.*

Proof. Let us consider the n-dimensional reduced diagram $g : (D^n, S^{n-1}) \to \widetilde{X}$ (Definition 3.14). Let $\tau \in \widetilde{X}$ be the $(n-1)$-cell such that $i(\tau) = \sigma_1$ and $t(\tau) = \sigma_2$, for $\sigma_1, \sigma_2 \in D$. In terms of poset $\mathcal{P}$, $\tau \subset \sigma_1$ and $\tau \subset \sigma_2$ where σ_1, σ_2 are n-cells in $\widetilde{X}$ with the property that $\sigma_1, \sigma_2 \in D(\subset V_\Gamma)$ and also $\phi_D(\sigma_1) \neq \phi_D(\sigma_2)$.

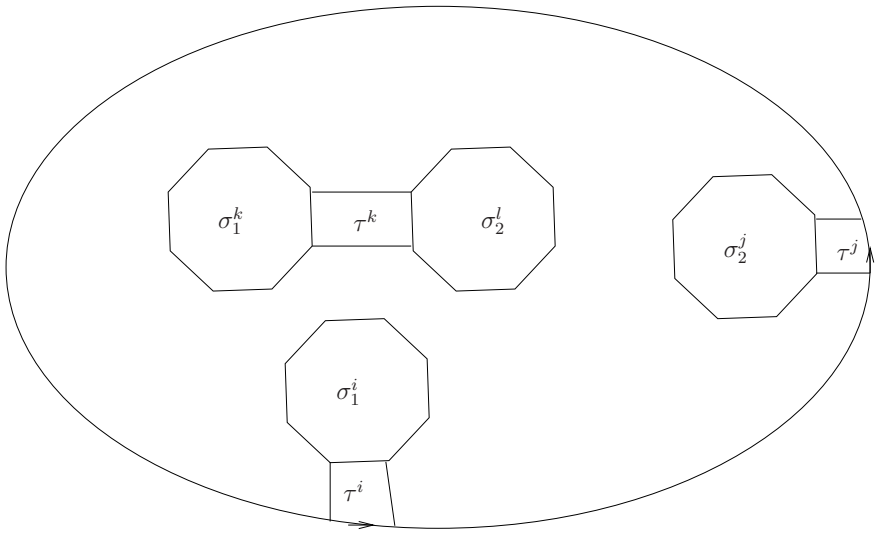

Figure 5.1: 2-diemnsional example with pre-images σ_1 , σ_2 and 1-cell τ in (D^2, S^1)

By the definition of ϕ_D, there are $\phi_D(\sigma_1)$ 0-handles in (D^n, S^{n-1}) that map onto σ_1 via g and similarly there are $\phi_D(\sigma_2)$ 0-handles in (D^n, S^{n-1}) that map onto σ_2 via g. Next, as we have $\phi_D(\sigma_1) \neq \phi_D(\sigma_2)$, this implies τ is one of the

$(n-1)$-cells forming the boundary $(n-1)$-sphere, i.e, $\tau \in \partial_V D$ and as both n-cells have more than one pre-images, thus, τ too has one or more pre-images in (D^n, S^{n-1}) associated with pre-images of both σ_1 and σ_2. The pre-images of σ_1 and σ_2 are either in the interior of (D^n, S^{n-1}) with pre-images of τ or they are at the boundary with τ as a boundary $(n-1)$-cell in some instances. If all the pre-

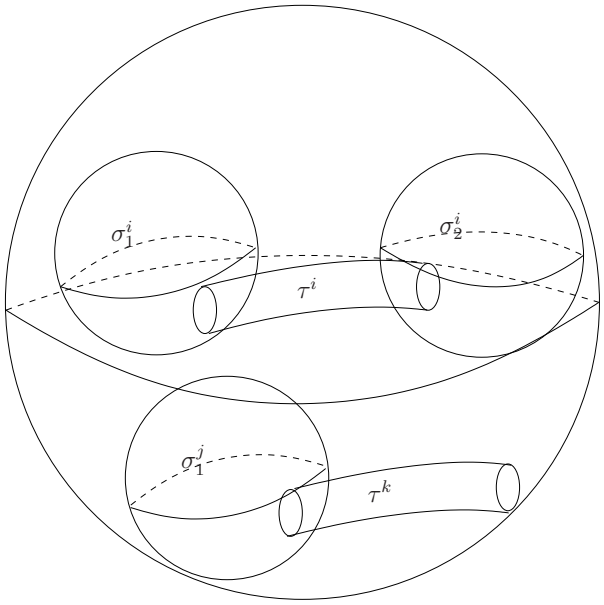

Figure 5.2: 3-diemnsional example with pre-images for cells σ_1 , σ_2 and 2-cell τ in (D^3, S^2)

images of σ_1 and σ_2 are in the interior of (D^n, S^{n-1}) with all pre-images of τ in the interior, then this implies $\phi_D(\sigma_1) = \phi_D(\sigma_2)$, which is against our assumption.

Without loss of generality let us assume that $\phi_D(\sigma_1) > \phi_D(\sigma_2)$. In this case if at most $\phi_D(\sigma_2)$ of the pre-images are in the interior of (D^n, S^{n-1}), then as we are considering handle decomposition of n-balls which are manifolds, the only way a pre-image of σ_2 appears in the interior is if it is accompanied with a pre-image of σ_1 and they share a pre-image of τ which is a 1-handle. Figures 5.1 and 5.2 are illustrations of this in two and three dimensions, where τ^i denotes a pre-image

of τ while σ_k^i etc. denotes the pre-images of σ_k for $k = 1, 2$. In this figure, one pre-image of τ, a 1-handle, is in the interior of (D^n, S^{n-1}) between pre-images of σ_1 and σ_2 which are both 0-handles, while the other is at the boundary adjoined to the 0-handle which is another pre-image of σ_1 . This implies that at least $(\phi_D(\sigma_1) - \phi_D(\sigma_2)) = (\phi_D(i(\tau) - \phi_D(t(\tau))$ of the pre-images of σ_1 are at the boundary of (D^n, S^{n-1}) with τ as a boundary $(n-1)$-cell.

Thus, $|\partial D^n| \geq \sum_{\tau \in \partial_V D} |\phi_D(i(\tau) - \phi_D(t(\tau)|$ which implies, $\| \nabla \phi_D \| \leq |\partial D^n|$. $\square$

Remark 5.14. At this point the problem involving the volume of the balls $Vol^n(D^n)$ and the area or volume of the boundary sphere $|\partial D^{n-1}|$, has reduced to one involving $||\phi_D||$ and $||\nabla \phi_D||$. In the next chapter we are going to use Varopoulos transport argument to prove the isoperimetric inequality involving $||\phi_D||$ and $||\nabla \phi_D||$. In case of the group $\mathcal{H}$ we will show that $||\phi_D|| \leq const.||\nabla \phi_D||^{\frac{4}{3}}$ and in the case of $\mathcal{S}$, we will show that $||\phi_D|| \preceq const.||\nabla \phi_D|| \ln(||\nabla \phi_D||)$. These inequalities automatically provide upper bounds for the second order Dehn functions in both cases.

Chapter 6

Upper Bounds- Varopoulos Transport Argument

In this section we are going to use Varopoulos transport to obtain isoperimetric inequalities in case of groups $\mathcal{H}$ and $\mathcal{S}$. We are going to consider reduced diagrams, since in case they are unreduced we can always use Proposition 3.14 from Section 3.2 to obtain a reduced diagram. As before, we will denote the volume (or area) of an n-ball by $|D^n|$ and the volume (or area) of its boundary by $|\partial D^n|$, for any n.

The Varopoulos isoperimetric inequality and Dehn functions have very little in common with each other. The only cases where they appear likely to agree are when the groups are fundamental groups of manifolds and also we are considering only top dimensional Dehn functions. So, in the cases we have here we can apply Varopoulos transport to obtain the isoperimetric ineqaulity and hence the upper bounds of second order Dehn functions. Here is a short discussion on this connection between the two concepts.

6.1 The connection between Dehn functions and Varopoulos Isoperimetric Inequalities

Varopoulos isoperimetric inequality was discussed by Varopoulos in [39]. One of his inspirations for looking at groups as geometric objects was Milnor's 1968 paper [29]. In this paper Milnor had showed that the fundamental group of a negatively curved compact manifold is of exponential growth. But the fundamental group of any compact manifold is finitely generated, hence the interest in finitely generated groups. Let the group G be generated by $g_1, g_2, ..., g_k$. A ball of radius n, centered at the identity $e \in G$, was the set of group elements of the form $g = g_{i_1}^{\varepsilon_1} g_{i_2}^{\varepsilon_2} .... g_{i_p}^{\varepsilon_p}$ where, $0 \leq p \leq n$, $1 \leq i_\alpha \leq k$ and $\varepsilon_\alpha = \pm 1$. The number of elements in the n-ball, is denoted by γ_n, and is known as the growth function of the group G. After Milnor's work the growth in volume of these groups were studied in details and in 1981 Gromov ([20]) gave an algebraic characterization of groups that satisfied $\gamma_n = \mathcal{O}(n^A)$, for some fixed $A \geq 0$. This automatically raised the question to consider the isoperimetric inequalities on finite subsets of G and Varopoulos showed that it was a valid question. He showed that, if $\Omega \subset G$ is finite and the boundary of Ω is $\partial\Omega = \{\omega \in \Omega \mid d(\omega, G \backslash \Omega) \leq 1\}$, then for $A \geq 1$,

$$Card(\Omega)^{\frac{A-1}{A}} \leq C\, Card(\partial\Omega) \qquad (*)$$

($C > 0$ and $Card(.)$ denotes the cardinality of a set) implied that $\gamma_n \geq C_1 n^A$. The converse of this implication was also proved by him in the same article. The isoperimetric inequality $(*)$ is referred to as Varopoulos isoperimetric inequality in this context.

It should be noted here that there is no connection between this classical

isoperimetric inequality and Dehn functions mentioned above except for a special case. We will illustrate this fact about the lack of connection between the two with examples given below. Both these examples are groups of exponential growth and we use the following result by Coulhoun and Saloff-Coste ([15]) to show that the Dehn function and the isoperimetric inequality by Varopoulos do not match in these cases.

Theorem 6.1 (Coulhoun and Saloff-Coste, [15]). *Given a finitely presented group G, let $\{g_1, g_2, ..., g_k\}$ be a finite generating set. For any finite subset Ω of G we define the boundary of Ω by $\partial\Omega = \{x \in \Omega \mid \exists i \in \{1, ..., k\}$ and $\epsilon = \pm 1$ such that $xg_i^{\epsilon} \in \Omega^c\}$. Then, if $V(n) = |B(n)|$ is the function of growth, (where $B(n) = \{x \in G \mid x = g_{i_1}^{\epsilon_1} ... g_{i_n}^{\epsilon_n}, i_1, ..., i_n \in \{1, 2, ..., k\}, \epsilon_j = 0, \pm 1\}$ is the ball of radius n) and $V(n) \geq Ce^{cn^{\alpha}}, 0 < \alpha \leq 1$ we have $|\Omega|(\log|\Omega|)^{-1/\alpha} \leq C\,|\partial\Omega|$.*

Example 6.2. Let us consider the group $F_2 \times \mathbb{Z}$, where F_2 denotes the free group on two generators. The ordinary (first order) Dehn function for this group is given by $\delta(x) \sim x^2$ (please refer to Brick's article [10] for the details). But this group has exponential growth which is clear if one looks at the universal cover in this case which is $T \times \mathbb{R}$ where T represents an infinite four-valent tree (the universal cover corresponding to F_2). In case of $F_2 \times \mathbb{Z}$, $V(n) \geq 4^n = e^{\ln(4)n}$ which implies that $\alpha = 1$. Therefore, using Theorem 6.1 above we have the following isoperimetric inequality, $\frac{|\Omega|}{(\log|\Omega|)} \leq C\,\partial|\Omega|$.

Since $\ln(x) < x^{1/p}$ for any positive integer p, we choose a positive integer $p > 2$ say and then, $|\Omega|^{\frac{p-1}{p}} \leq C'\,|\partial\Omega|$, which implies, $|\Omega| \leq C''\,|\partial\Omega|^{\frac{p}{p-1}}$.

Example 6.3. Next let us consider the following presentation for the Baumslag Solitar group $BS(1, 2)$, $\mathcal{P} = \{a, t \mid tat^{-1} = a^2\}$. In this case too the group has exponential growth and the Dehn function is $\delta(x) \sim 2^x$ (please refer to Bridson's

article in [13] for the proof). Next we can check by looking at the Bass-Serre tree that $V(n) \geq 3^{\frac{n}{2}}$ which implies that $\alpha = 1$. The Bass-Serre tree can be obtained by collapsing each segment in the universal cover (Figure 6.1) to a point and each strip of 2-cells to an edge and it turns out to be a tri-valent tree in this case and so $|V(2n)| \geq 3^n$ hence, $|V(n)| \geq 3^{\frac{n}{2}} = e^{\ln(3)\frac{n}{2}}$.

Therefore, $\frac{|\Omega|}{(\log|\Omega|)} \leq C\,\partial|\Omega|$ for a finite subset $\Omega \subset BS(1,2)$. Again since $\ln(x) < \sqrt{x}$, so $|\Omega|^{\frac{1}{2}} \leq C'\,|\partial\Omega|$, which implies, $|\Omega| \leq C'^2\,|\partial\Omega|^2$.

The reason for the difference in the Dehn function and the isoperimetric inequality can be attributed to the structure of the space associated to the group. If we take a look at the Cayley complex of this group we notice that the structure is not locally like a manifold as there is a noticeable branching in the universal cover (Figure 6.1). At each level, there are three horizontal strips made up of 2-cells, that joined along one segment. This means that the Varopoulos boundary defined above is larger compared to the boundary of the discs considered for the Dehn function.

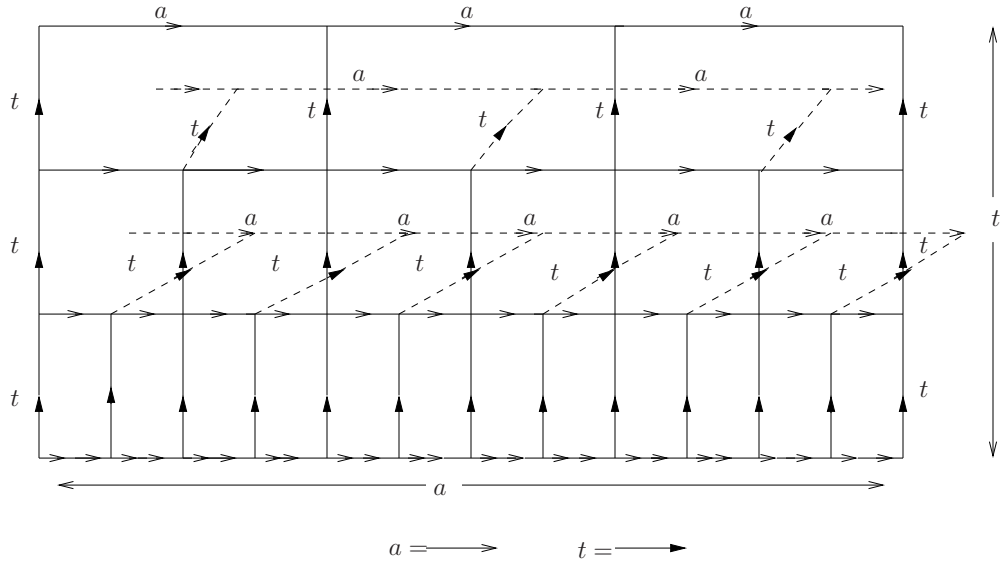

Figure 6.1: Portion of Cayley complex of $BS(1,2)$

However, if we have a group $G = \pi_1(M^n)$ where M^n represents an n-manifold then there should be a correspondence between the top dimensional Dehn function ($\delta^{(n-1)}$) and the Varopoulos isoperimetric inequality of the group G. In this thesis our main aim was to obtain (upper) bounds for second order Dehn functions for lattices of the Nil and Sol geometries using Varopoulos's isoperimetric inequality by considering dual graphs in the universal covers of the complexes corresponding to these groups.

6.2 Intuition behind the Varopoulos argument

In this section, we present the intuition behind the notion of transportation of mass from a finite-volume subset of a space. It is important to note here that all our examples are finitely presented groups and the space under consideration will be the universal covers associated to the groups.

The following argument is originally due to Varopoulos [39]. It was used by Gromov in [25] to demonstrate the transportation of mass (volume) in $\mathbb{R}^n$ and also that of a finite subset of group. This notion of transport was first described by Varopoulos in [39], where he described transport in association with random walks. The same argument was further discussed by Gromov in [25]. Gromov also used this argument in his paper on Carnot-Carathéodory spaces [24]. The lemma here is appropriately called "Measure Moving lemma" and helps in the proof of isopermetric inequalities of hypersurfaces in Carnot-Carathéodory manifolds. Before going into the technical details of the argument in Section 6.3, we will sketch the idea behind the argument and the reason it works, in this section.

Given a graph Γ let D be a finite subset of the vertices of the graph transported by a path γ, then the amount of mass transported through the boundary of D is

obviously bounded above by $(|\gamma| vol(\partial D))$. But we have to find a particular γ to bound $vol(D)$ by $vol(\partial D)$, for this we compute average transport. Transport of D corresponding to some γ is defined as the mass of D that is moved out of D by the action of γ. In other words it is the number of vertices in the set $(D\gamma \setminus D)$, where $D\gamma = \{v\gamma \mid v \in D\}$.

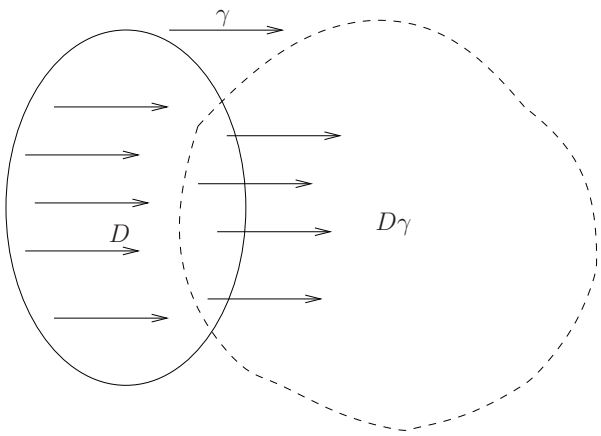

Figure 6.2: Transport of D

Next for the lower bound for the transport we have to show that it is possible to move a percentage of the set D off it. It is always possible to choose the path γ such that l_γ is large enough that almost all of D is transported off itself, but the key is to find a γ in the graph such that it is small enough and moves at least half of D off itself. Since the shape of D maybe very unpredictable Figure 6.3, therefore transport via a path α maybe very small compared to the mass of D again for another path γ the transport maybe very large. In order to solve this problem we bound the length of the path by considering a ball of radius R in Γ, denoted by $B(R)$ such that $|B(R)| \approx 2|D|$ and taking the average transport over all $\gamma \in B(R)$. Once we show that the average transport is at least half of D, we know that there is at least one path γ_0 such that the transport of D via γ_0

is at least half of the mass of D. This inequality in turn leads to the respective isoperimetric inequalities of the groups we discuss in this context.

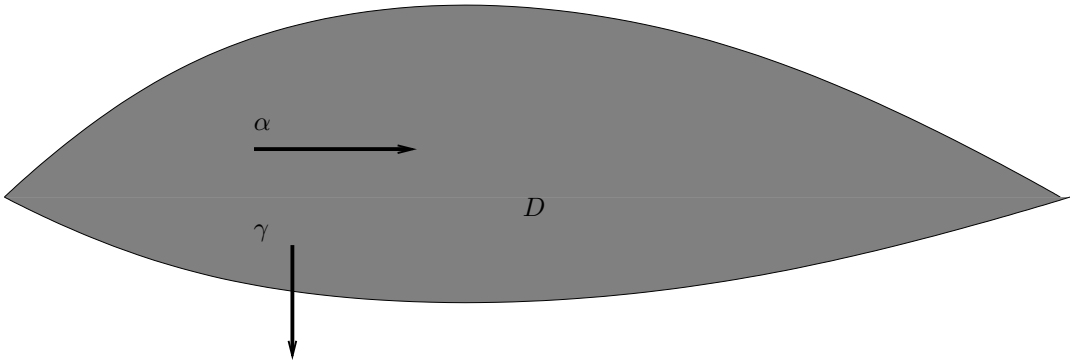

Figure 6.3: Transport of D with α is small compared to the mass of D while that with respect to γ is large compared to D

6.3 The Transport Computation

Given a finitely presented group G, let the Γ be the dual Cayley graph (defined in Section 5.2.1) corresponding to the universal cover of n-complex X corresponding to G. This graph is infinite but it is locally finite. The edges are directed and labelled, also there is only one outgoing (incoming) edge with a given label at any vertex. Γ is a Cayley graph with respect to the presentation of the groups defined in Section 5.2. Also the graph is endowed with the path metric and each edge is isomorphic to the unit interval $[0, 1]$.

As defined in the previous section, in the following discussion the vertex set of Γ will be denoted by V_Γ and edge set by E_Γ. Next, consider the subset D in V_Γ corresponding to the n-cells in the image of $f : (D^n, S^{n-1}) \to X$. Let us consider the case when f is an embedding. Then we denote the map ϕ_D by the characteristic function $\chi_D : V_\Gamma \to \{0, 1\}$ defined by $\chi_D(\sigma) = 1$ when $\sigma \in D$,

otherwise $\chi_D(\sigma) = 0$. In this case $||\chi_D|| = |D|$, where $|D|$ denotes the number of vertices in D.

Next, $\nabla\chi_D : \partial_V D \to \{0, 1\}$ is defined in the following way,

$\nabla\chi_D(\tau) = |\chi_D(t(\tau)) - \chi_D(i(\tau))|$, where $i, t : E_\Gamma \to V_\Gamma$ gives the initial and terminal vertices respectively of any edge in E_Γ.

Therefore, $|\partial_V D| = \sum_{\tau \in \partial_V D} |\chi_D(t(\tau)) - \chi_D(i(\tau))|$.

Let $\gamma \in B(r) \subset \Gamma$, where $B(r)$ represents a ball of radius r in the graph. We choose r large enough such that $|B(r)| \geq 2|D| > |B(r-1)|$.

Varopoulos Transport $T_D^\gamma = |D\gamma \setminus D|$

Average Transport $\widehat{T_D^\gamma} = \frac{1}{|B(r)|} \sum_{\gamma \in B(r)} T_D^\gamma$.

Proposition 6.4 (Varopoulos, [39]). $\widehat{T_D^\gamma} \geq \frac{1}{2}|D|$.

Proof. $\widehat{T_D^\gamma} = \frac{1}{|B(r)|} \sum_{\sigma,\gamma} |\{(\sigma, \gamma) \mid \sigma \in D,\ \sigma\gamma \in (V_\Gamma \setminus D),\ \gamma \in B(r)\}|$

$$= \frac{1}{|B_1(r)|} \sum_{\gamma \in B(r)} \sum_{\sigma \in D} (\chi_D(\sigma) - \chi_D(\sigma\gamma))$$

$$= \sum_{\sigma \in D} \frac{1}{|B(r)|} \sum_{\gamma \in B(r)} (\chi_D(\sigma) - \chi_D(\sigma\gamma))$$

$$= \sum_{\sigma \in D} \left(\frac{|B(r)|}{|B(r)|} \chi_D(\sigma) - \frac{\sum_\gamma \chi_D(\sigma\gamma)}{|B(r)|} \right)$$

$$= \sum_{\sigma \in D} \left(1 - \frac{|B_\sigma(r) \cap D|}{|B(r)|}\right), \text{ where } B_\sigma(r) \text{ is a ball of radius } r \text{ at vertex } \sigma.$$

But since we assumed that $|B(r)| \ > 2|D|$, so we have,

$$\widehat{T_D^\gamma} \ \geq \ \sum_{\sigma \in D}(1 - \frac{1}{2}),$$

$$\text{or, } \ \widehat{T_D^\gamma} \ \geq \ \tfrac{1}{2}|D|$$

So there is $\gamma_0 \in B_1(r)$ such that $T_D^{\gamma_0} \geq \frac{|D|}{2}$.

□

Next we obtain an upper bound for the transport T_D^γ in the following proposition.

Proposition 6.5. *$T_D^\gamma \ \leq \ l_\gamma \ |\partial_V D|$; where l_γ is the length of γ.*

Proof. The path corresponding to the word γ can be expressed as a sequence of the generators in Γ, namely, $a_1 a_2 a_3 ....a_{l_\gamma}$ where $a_i = \alpha^{\pm 1}$ or $= \beta^{\pm 1}$ for $1 \leq i \leq l_\gamma$.

***Notation*:** Let $a_1 a_2 ...a_k = \alpha_k$ for $1 \leq k \leq l_\gamma$ and α_0 is the identity of the group.

The Varopoulos Transport as defined before is,

$$\begin{aligned} T_D^\gamma \ &= \ |D\gamma \setminus D| \\ \therefore T_D^\gamma \ &= \ \sum_{\sigma \in D} |\{(\sigma, \gamma) \ | \ y \in D, \ \sigma\gamma \in (V_\Gamma \setminus D), \ \gamma \in B_1(r)\} \ | \\ &= \ \sum_{\sigma \in D} \ |\chi_D(\sigma) - \chi_D(\sigma\gamma)| \end{aligned}$$

Now using the sequence and notation defined above, we can write,

$$T_D^\gamma \ \leq \ \sum_{\sigma \in D} \ \left(\sum_{i=1}^{l_\gamma} |\chi_D(\sigma\alpha_i) - \chi_D(\sigma\alpha_{i-1})| \right)$$

So in the inner sum, in the expression above, the terms have value either 0 or 1, the terms which have value 1, represent boundary edges.

In order to establish the upper bound for the transport of D by $\gamma \in \Gamma$, we will show that each of the boundary edge mentioned above appears at most l_γ times in the sum. So, we start with the transport of a vertex $\sigma_i \in D$ via the path γ. Let us denote the edge between the vertices $\sigma_i\alpha_{j-1}$ and $\sigma_i\alpha_j$ by τ where $1 \leq j \leq l_\gamma$. Now let us express the path γ as the sequence $\gamma_1\tau\gamma_2$; where γ_1, γ_2 are two sub-paths of γ such that the initial vertex of γ_1 is σ_i while the terminal vertex of γ_2 is $\sigma_i\gamma$, and τ is the label of the jth edge of γ. Then, by uniqueness of path liftings in a Cayley graph, it is known that γ_1 and γ_2 are both unique with respect to initial vertex σ_i. In other words, the paths corresponding to γ originating from vertices of D other than σ_i, do not have τ as the jth edge. So if the path γ originating from vertex $\sigma_j \in D$, (where $\sigma_j \neq \sigma_i$), can be expressed as $\gamma_3\tau\gamma_4$, then, here τ is the label for say the $k^{th}, (k \neq j)$ edge of this path while γ_3 and γ_4 are both unique sub-paths with respect to σ_j. So a particular edge in path γ can appear at most l_γ times.

Therefore, $T_D^\gamma \leq l_\gamma \sum_{\sigma_i,\sigma_j \in V_\Gamma} |\chi_D(\sigma_i) - \chi_D(\sigma_j)|$.

So, $T_D^\gamma \leq l_\gamma \ |\partial_V D|$. □

Next we will consider $f : (D^n, S^{n-1}) \to X$ to be an immersion, and so instead of a characteristic function we consider a non-negative, integer-valued function ϕ_D (Definition 5.9) and show that the Varopoulos argument works in this case too. Assume as before, that $\gamma \in B_1(r) \subset G$, where $B_1(r)$ represents a ball of radius r centered at the identity in the graph. We choose r large enough such that $|B_1(r)| \geq 2 \parallel \phi_D \parallel > |B_1(r-1)|$.

Varopoulos Transport $T_D^\gamma = \sum_{\sigma \in D} |\phi_D(\sigma) - \phi_D(\sigma\gamma)|$.

$\therefore$ Average Varopoulos Transport is given by,

$$\widehat{T_D^\gamma} \;=\; \tfrac{1}{|B_1(r)|} \sum_{\gamma \in B_1(r)} T_D^\gamma \; .$$

Remark 6.6. The definitions of $||\phi_D||$, $||\nabla \phi_D||$ used below can be found as Remark 5.10 and Definition 5.12 respectively in Section 5.2.1

Proposition 6.7 (Calhoun, Saloff-Coste, [15])**.** $\widehat{T_D^\gamma} \geq \frac{1}{2}||\phi_D||$

Proof.

$$\begin{aligned}
\widehat{T_D^\gamma} = \; & \tfrac{1}{|B_1(r)|} \sum_{\gamma \in B_1(r)} \sum_{\sigma \in D} |\phi_D(\sigma) - \phi_D(\sigma\gamma)| \\
= \; & \sum_{\sigma \in D} \frac{1}{|B_1(r)|} \sum_{\gamma \in B_1(r)} |\phi_D(\sigma) - \phi_D(\sigma\gamma)| \\
\geq \; & \sum_{\sigma \in D} \frac{1}{|B_1(r)|} \sum_{\gamma \in B_1(r)} |\phi_D(\sigma)| - |\phi_D(\sigma\gamma)| \\
\geq \; & \sum_{\sigma \in D} \frac{1}{|B_1(r)|} \left(|B_1(r)| \phi_D(\sigma) - \sum_{\gamma \in B_1(r)} \phi_D(\sigma\gamma) \right) \\
\geq \; & \sum_{\sigma \in D} \left(\phi_D(\sigma) - \frac{1}{|B_1(r)|} \sum_{\gamma \in B_1(r)} \phi_D(\sigma\gamma) \right)
\end{aligned}$$

Since, $\sum_{\gamma \in B_1(r)} \phi_D(\sigma\gamma) \;\leq\; \| \phi_D \|$, we have,

$$\widehat{T_D^\gamma} \;\geq\; \sum_{\sigma \in D} \left(\phi_D(\sigma) - \frac{\| \phi_D \|}{|B_1(r)|} \right)$$

According to our initial assumption, $\frac{\|\phi_D\|}{|B_1(r)|} \leq \frac{1}{2}$, and that implies, $\frac{\|\phi_D\|}{|B_1(r)|} \leq \frac{\phi_D(\sigma)}{2}$, for any particular $\sigma \in D$.

$$\therefore \widehat{T_D^\gamma} \;\geq\; \sum_{\sigma \in D} \frac{\phi_D(\sigma)}{2} = \frac{1}{2} \| \phi_D \|$$

In particular, $\exists \gamma_0 \in B_1(r)$ such that, $T_D^{\gamma_0} \geq \frac{\|\phi_D\|}{2}$. $\square$

Proposition 6.8. *$T_D^{\gamma} \leq l_\gamma ||\nabla \phi_D||$, where l_γ denotes the length of the path/word γ.*

Proof. We will use the same argument as in proof of Lemma 6.5 to show this. The path corresponding to the word γ can be expressed as before by a sequence of the generators in Γ, namely, $a_1 a_2 a_3 .... a_{l_\gamma}$ where $a_i = \alpha^{\pm 1}$ or $= \beta^{\pm 1}$ for $1 \leq i \leq l_\gamma$.

***Notation*:** Let $a_1 a_2 ... a_k = \alpha_k$ for $1 \leq k \leq l_\gamma$ and α_0 is the identity of the group.

The Varopoulos Transport as defined before is,

$$\begin{aligned} T_D^{\gamma} &= |D\gamma \setminus D| \\ \therefore T_D^{\gamma} &= \sum_{\sigma \in D} |\phi_D(\sigma) - \phi_D(\sigma\gamma)| \end{aligned}$$

As before,

$$T_D^{\gamma} \leq \sum_{\sigma \in D} \left(\sum_{i=1}^{l_\gamma} |\phi_D(\sigma\alpha_i) - \phi_D(\sigma\alpha_{i-1})| \right)$$

The terms in the inner sum are either zero or a natural number. In the case when they are non-zero, they represent boundary edges in the Varopoulos sense.

So as in the proof of Lemma 6.5, each of these afore-mentioned boundary edges appear in the sum at most l_γ times. Therefore,

$$T_D^{\gamma} \leq l_\gamma \sum_{\sigma_i \sigma_j \in V_\Gamma} |\phi_D(\sigma_i) - \phi_D(\sigma_j)|,$$

which means, $T_D^{\gamma} \leq l_\gamma \parallel \nabla \phi_D \parallel$. $\square$

6.4 Isoperimetric Inequalities for groups of Polynomial growth

6.4.1 A 2-dimensional Example

Here we will discuss the 2-dimensional example $\mathbb{Z}^2$. Let us consider the presentation $\langle a, b \mid [a, b]\rangle$ for $\mathbb{Z}^2$. Let $\widetilde{X}$ be the universal cover of the 2-complex X corresponding to the presentation given above for $\mathbb{Z}^2$. As before let us denote a ball of radius r centered at the identity in $\widetilde{X}$ by $B_1(r)$.

Let us choose r such that $|B_1(r)| \geq 2||\phi_D|| > |B_1(r-1)|$. Also, $|B_1(r)| \sim \mathcal{O}(r^2)$.

From the propositions above, we already know that:

$\frac{1}{2}||\phi_D|| \leq T_D^{\gamma_0} \leq l_{\gamma_0} |\partial_V D|$ for some $\gamma_0 \in B_1(r)$.

$$\therefore ||\phi_D|| \leq 2l_{\gamma_0} ||\nabla\phi_D||$$

$$\therefore ||\phi_D|| \preceq ||\phi_D||^{\frac{1}{2}} |||\nabla\phi_D|| \text{ ; since } l_{\gamma_0} \leq r$$

$$\therefore ||\phi_D|| \preceq ||\nabla\phi_D||^2$$

When the 2-disc along with its boundary circle is embedded in $\widetilde{X}$ via the transverse map $f : (D^2, S^1) \to \widetilde{X}$, $||\nabla\phi_D|| = |\partial D^2|$. On the other hand, in the case when we have a reduced diagram $f : (D^2, S^1) \to \widetilde{X}$, such that the disc and its boundary are not embedded, then by Lemma 5.13 $||\nabla\phi_D|| \leq |\partial D^2|$. Hence we have the following isoperimetric inequality.

$$\therefore ||\phi_D|| \preceq ||\nabla\phi_D||^2 \leq (2Const.)^2 |\partial D^2|^2.$$

$$\therefore Vol^2(D^2) \preceq |\partial D^2|^2.$$

6.4.2 A 3-dimensional Example

In this section we present the an upper bound for the second-order Dehn functions of the 3-dimensional group $\mathcal{H}$ and consequently all cocompact lattices in the Nil geometry. In other words we complete the proof of Theorem 1.1 here.

Lemma 6.9. $||\phi_D|| \preceq ||\nabla\phi_D||^{\frac{4}{3}}$

Proof. Let Γ denote the dual Cayley graph embedded in $\widetilde{X}$ corresponding to the generating set $\mathcal{A}_0$ defined in Lemma 5.6 part (i) where $\widetilde{X}$ is the universal cover of the 3-complex corresponding to $\mathcal{H}$. Let us consider the reduced 3-dimensional diagram $f : (D^3, S^2) \to \widetilde{X}$ (defined in Section 3.2). Let D be the finite set of vertices in Γ dual to the 0-handles present in the diagram mentioned above.

Next, let us choose a ball of radius r in the graph Γ such that $|B_1(r)| \geq 2||\phi_D|| > |B_1(r-1)|$, where $K > 2$ is real and K is sufficiently large. Also, $|B_1(r)| \sim \mathcal{O}(r^4)$, by Lemma 4.5.

From Section 6.3, we already know that, $\frac{1}{2}||\phi_D|| \leq T_D^{\gamma_0} \leq l_{\gamma_0}\ |\partial_V D|$ for some $\gamma_0 \in B_1(r)$. Also as $l_{\gamma_0} \leq r$ and $r - 1 \leq (2||\phi_D||)^{\frac{1}{4}} \Rightarrow r \preceq (||\phi_D||)^{\frac{1}{4}}$ and we have the following,

$$\begin{aligned}
&\therefore ||\phi_D|| \leq 2l_{\gamma_0}\ ||\nabla\phi_D|| \\
&\therefore ||\phi_D|| \preceq 2||\phi_D||^{\frac{1}{4}}\ ||\nabla\phi_D|| \\
&\therefore ||\phi_D|| \preceq ||\nabla\phi_D||^{\frac{4}{3}}.
\end{aligned}$$

□

Given a reduced diagram $f : (D^3, S^2) \to \widetilde{X}$, if the 3-ball and its boundary sphere are embedded in $\widetilde{X}$, then $||\nabla\phi_D|| = |\partial D^3|$. If they are not embedded then by Lemma 5.13, $||\nabla\phi_D|| \leq |\partial D^3|$. Hence we have the following inequality. $\therefore Vol^3(D^3) \preceq |\partial D^3|^{\frac{4}{3}}$, where $|\partial D^3|$ is the volume of the boundary sphere.

Therefore, by the definition of $\delta^{(2)}$, if x is the maximum number of 3-cells in the boundary sphere, then $\delta^{(2)}(x) \preceq x^{\frac{4}{3}}$.

6.5 Isoperimetric Inequalities for groups of Exponential growth

In this section we present the upper bound for the second-order Dehn functions of $\mathcal{S}$ and consequently all cocompact lattices in the Sol geometry. In other words, the proof of Theorem 1.2 will be completed here.

Lemma 6.10. $||\phi_D|| \preceq \ln(||\nabla\phi_D||)\ ||\nabla\phi_D||$.

Proof. We start with a reduced 3-dimensional diagram (D^3, S^2), corresponding to a finitely presented group G. In this sub-section, we have a 3-dimensional example with exponential growth namely, the solvable group $\mathcal{S}$.

Let us choose r such that $|B_1(r)| \geq 2||\phi_D|| > |B_1(r-1)|$, $|B_1(r)| \sim Ce^{\ln(k)r}$, k, C are both positive constants,(by Lemma 4.8). Therefore we have,

$$||\phi_D|| \geq Ce^{\ln(k)r}.$$

$$\therefore r \preceq \ln(||\phi_D||)$$

Next, from Section 6.3, we already know that, $\frac{1}{2}||\phi_D|| \leq T_D^{\gamma_0} \leq l_{\gamma_0}\ ||\nabla\phi_D||$ for some $\gamma_0 \in B_1(r)$.

$$\therefore ||\phi_D|| \leq 2l_{\gamma_0}\ ||\nabla\phi_D||$$

$$\therefore ||\phi_D|| \preceq \ln(||\phi_D||)\ ||\nabla\phi_D|| \text{ ; since } l_{\gamma_0} \leq r \qquad (*)$$

As in the case of $\mathcal{H}$, we can say the in the embedded case $||\nabla\phi_D|| = |\partial D^3|$, while in the immersed case we have $||\nabla\phi_D|| \leq |\partial D^3|$, using the Lemma 5.13 above. Hence we have the following isoperimetric inequality,

Taking natural logarithm, ln, on either side of $(*)$ we get,

$$\ln(||\phi_D||) \preceq \ln(\ln(||\phi_D||)\ ||\nabla\phi_D||),$$

$$\therefore \ln(||\phi_D||) \preceq \ln(\ln(||\phi_D||) + \ln(||\nabla\phi_D||),$$

Now from $(*)$,for large values of $||\phi_D||$,

$$\ln(||\phi_D||) \leq \frac{||\phi_D||}{\ln(||\phi_D||)} \preceq ||\nabla\phi_D||,$$

$$\therefore \ln(||\phi_D||) \ \preceq \ \ln(||\nabla\phi_D||)$$

Again from $(*)$,

$$||\phi_D|| \ \preceq \ \ln(||\nabla\phi_D||)\ ||\nabla\phi_D||. \qquad \square$$

From the lemma above we have, $Vol^3(D^3) \ \preceq \ \ln(|\partial D^3|)\ |\partial D^3|$, where $|\partial D^3|$ is the volume of the boundary sphere. Therefore, by the definition of $\delta^{(2)}$, if x is the maximum number of 3-cells in the boundary spheres then $\delta^{(2)}(x) \preceq x\ln(x)$.

Bibliography

[1] A.D. Alexandrov. A theorem on triangles in a metric space and some of its applications. *Trudy Mat. Inst. Steklov*, 38:5–23, 1951.

[2] J. M. Alonso, W. A. Bogley, R. M. Burton, S. J. Pride, and X. Wang. Second order Dehn functions of groups. *Quart. J. Math. Oxford Ser. (2)*, 49(193):1–30, 1998.

[3] J.M. Alonso, X Wang, and S.J. Pride. Higher-dimensional isoperimetric (or Dehn) functions of groups. *Journal Group Theory*, (2):81–112, 1999.

[4] Juan M. Alonso. Inégalités isopérimétriques et quasi-isométries. *C. R. Acad. Sci. Paris Sér. I Math.*, 311(12):761–764, 1990.

[5] J.-C. Birget, A. Yu. Ol'shanskiĭ, E. Rips, and M. V. Sapir. Isoperimetric functions of groups and computational complexity of the word problem. *Ann. of Math. (2)*, 156(2):467–518, 2002.

[6] N. Brady, M. Bridson, M. Forester, and K. Shankar. Snowflake groups, Perron-Frobenius eigenvalues, and isoperimetric spectra. *Geometry and Topology*, 2009.

[7] N. Brady and M. R. Bridson. There is only one gap in the isoperimetric spectrum. *Geom. Funct. Anal.*, 10(5):1053–1070, 2000.

[8] N. Brady and M. Forester. Density of Isoperimetric Spectra. *Preprint*, 2008.

[9] N. Brady, T. Riley, and H. Short. *The geometry of the word problem for finitely generated groups*. Advanced Courses in Mathematics. CRM Barcelona. Birkhäuser Verlag, Basel, 2007. Papers from the Advanced Course held in Barcelona, July 5–15, 2005.

[10] S. G. Brick. On Dehn functions and products of groups. *Trans. Amer. Math. Soc.*, 335(1):369–384, 1993.

[11] M. Bridson. Polynomial Dehn functions and the length of asynchronously automatic structures. *Proc. London Mathematical Society*, 85(3):441–466, 2002.

[12] M. Bridson and A. Haefliger. *Metric Spaces of Non-Positive Curvature*, volume 319. Springer, 1999.

[13] M Bridson, S.M. Salamon, et al. *Invitations to Geometry and Topology*. Oxford Science Publications, 2002.

[14] S. Buoncristiano, C.P Rourke, and B.J Sanderson. A geometric approach to homology theory. *London Mathematical Society Lecture Note Series*, (18):iii+149, 1976.

[15] T Coulhon and L Saloff-Coste. Isoperimetrie pour les groupes et les varietes. *Revista matemática iberoamericana*, 9:293–314, 1993.

[16] M. Dehn. Über unendliche diskontunuierliche Gruppen. *Math. Ann.*, 71:116–144, 1912.

[17] D. Epstein, J. Cannon, D. Holt, S. Levy, M. S. Paterson, and W. P. Thurston. *Word processing in groups*. Jones and Bartlett Publishers, Boston, MA, 1992.

[18] M. Forester. Lecture Notes on Topological Methods in Group Theory.

[19] S. M. Gersten. Dehn functions and l_1-norms of finite presentations. 23:195–224, 1992.

[20] M. Gromov. Groups of polynomial growth and expanding maps. *Inst. Hautes Études Sci. Publ. Math.*, (53):53–73, 1981.

[21] M. Gromov. Filling Riemannian manifolds. *J. Differential Geom.*, 18(1):1–147, 1983.

[22] M. Gromov. *Hyperbolic groups*, volume 8 of *Math. Sci. Res. Inst. Publ.* Springer, New York, 1987.

[23] M. Gromov. *Asymptotic invariants of infinite groups*, volume 182 of *London Math. Soc. Lecture Note Ser.* Cambridge Univ. Press, Cambridge, 1993.

[24] M. Gromov. *Carnot-Carathéodory spaces seen from within*, volume 144 of *Progr. Math.* Birkhäuser, 1996.

[25] M. Gromov. *Metric Structures for Riemannian and Non-Riemannian Spaces*, volume 152 of *Progress in Mathematics*. Birkhauser, 1999.

[26] E. R. Van Kampen. On Some Lemmas in the Theory of Groups. *Amer. J. Math.*, 55(1-4):268–273, 1933.

[27] J. P. McCammond. A general small cancellation theory. *Internat. J. Algebra Comput.*, 10(1):1–172, 2000.

[28] J. Milnor. *Lectures on the h-cobordism theorem*. Notes by L. Siebenmann and J. Sondow. Princeton University Press, Princeton, N.J., 1965.

[29] J. Milnor. A note on curvature and fundamental group. *J. Differential Geometry*, 2:1–7, 1968.

[30] A. Yu. Ol'shanskiĭ. *Geometry of defining relations in groups*, volume 70 of *Mathematics and its Applications (Soviet Series)*. Kluwer Academic Publishers Group, Dordrecht, 1991. Translated from the 1989 Russian original by Yu. A. Bakhturin.

[31] P. Pansu. An isoperimetric inequality on the Heisenberg group. *Rend. Sem. Mat. Univ. Politec. Torino*, (Special Issue):159–174 (1984), 1983. Conference on differential geometry on homogeneous spaces (Turin, 1983).

[32] J. A. F Plateau. Statique Experimentale et Théorique des Liquides Soumis aux Seules Forces Moleculaires, 1873. Paris, Gauthier-Villars.

[33] E. Rips. Generalized small cancellation theory and applications. I. The word problem. *Israel J. Math.*, 41(1-2):1–146, 1982.

[34] C. P. Rourke and B. J. Sanderson. *Introduction to piecewise-linear topology*. Springer-Verlag, New York, 1972. Ergebnisse der Mathematik und ihrer Grenzgebiete, Band 69.

[35] M. V. Sapir, J. Birget, and E. Rips. Isoperimetric and isodiametric functions of groups. *Ann. of Math. (2)*, 156(2):345–466, 2002.

[36] S. Smale. Generalized Poincaré's conjecture on dimensions greater than four. *Annals of Mathematics*, 74:391–406, 1961.

[37] J. R. Stallings. Polyhedral homotopy-spheres. *Bull. Amer. Math. Soc.*, 66:485–488, 1960.

[38] W. P. Thurston. *Three-dimensional geometry and topology. Vol. 1*, volume 35 of *Princeton Mathematical Series*. Princeton University Press, Princeton, NJ, 1997. Edited by Silvio Levy.

[39] N. Th Varopoulos. Random walks and Browninan motion on manifolds. *Symposia Mathematica,(Cortona, 1984), Academic Press, New York*, pages 97–109, 1987.

[40] C. T. C. Wall. Finiteness conditions for CW-complexes. *Ann. of Math. (2)*, 81:56–69, 1965.

[41] X. Wang. Second order Dehn functions of split extensions of the form $\mathbb{Z}^2 \rtimes_\phi F$. *Comm. Algebra*, 30(9):4121–4137, 2002.

[42] X. Wang and S. J. Pride. Second order Dehn functions and HNN-extensions. *J. Austral. Math. Soc. Ser. A*, 67(2):272–288, 1999. Group theory.